CEAS Aeronautical Journal
https://doi.org/10.1007/s13272-026-00993-9

ORIGINAL PAPER

Tailplane sizing for LH2 aircraft families: commonality assessment and preliminary design trade-offs

Angel Garmilla Manzano[1] · Felix Fritzsche[1] · Daniel Silberhorn[1] · Salvatore Asaro[2]

Received: 17 February 2026 / Revised: 21 May 2026 / Accepted: 29 June 2026
© The Author(s) 2026

Abstract

Liquid hydrogen (LH2) aircraft concepts with rear-fuselage tanks often necessitate a larger horizontal tailplane (HTP) due to the increased centre of gravity longitudinal travel. However, most studies focus on point designs of individual aircraft. In contrast, conventional kerosene aircraft are typically developed as families that share a common empennage across multiple variants. Whether such empennage commonality is feasible for LH2 families remains largely unexplored. This paper therefore investigates the performance trade-offs associated. A preliminary design methodology is developed to size an aircraft, influencing the design of its tailplane, based on the definition of two potential shorter family variants. All aircraft are sized simultaneously, resulting in a family with a common empennage. When maintaining fuel capacity across a kerosene aircraft family, the smallest member serves as the design driver for tailplane dimensions, as its shorter fuselage results in a reduced tailplane lever arm. For LH2 families using the same strategy, the results revealed that the fuel penalty due to tailplane commonality is halved when compared to an analogous kerosene family. The effect of the shorter lever arm on the HTP area in the case of the smallest variant is compensated by a reduced centre of gravity longitudinal range resulting from the placement of the tanks. However, family design strategies that do not assume tank commonality, now present significant design challenges.

Keywords Conceptual aircraft design · Tailplane sizing · Liquid hydrogen aircraft · Aircraft samily concept

Abbreviations

AAIB	Air accidents investigation branch
CAD	Computer aided design
CFRP	Carbon fiber reinforced polymer
CG	Centre of gravity
CPACS	Common parametric aircraft configurations schema
DLR	German aerospace center
EIS	Entry into service
ER	Extended range
FWD	Forward
HTP	Horizontal tailplane
ISA	International standard atmosphere
ISO	Isometric
LE	Leading edge
S	Long, mid, and short family member
MAC	Mean aerodynamic chord
MFM	Mission fuel mass
MLI	Multi-layer insulation
MTOM	Maximum take-off mass
OEM	Operating empty mass
PAX	Passenger
RCE	Remote component environment
SL	Sea level
SMR	Short-medium range
TLAR	Top level aircraft requirement
TO	Take-off
TOC	Top-of-climb
TOFL	Take-off field length
VTP	Vertical tailplane

✉ Angel Garmilla Manzano
angel.garmillamanzano@dlr.de

[1] Institute of System Architectures in Aeronautics, German Aerospace Center, Hein-Saß-Weg 22, 21129 Hamburg, Germany

[2] Delft University of Technology, Kluyverweg 1, 2629 HS Delft, The Netherlands

Published online: 10 July 2026

1 Introduction

Liquid hydrogen (LH2) is emerging as a promising solution to achieve zero carbon emissions by 2050. Recent technological advances have renewed interest in LH2-powered aircraft [1, 2]. Numerous studies indicate that rear-fuselage tank concepts are among the most effective approaches for integrating LH2 into conventional tube-and-wing aircraft designs. As highlighted by Verstraete et al., these tanks offer superior gravimetric efficiency and lower integration mass penalties compared to alternative solutions [3–5]. A notable drawback is the requirement for a larger horizontal tailplane (HTP) relative to conventional kerosene aircraft, to ensure feasible operations [6]. The variable mass of rear-fuselage tanks significantly increases the aircraft's longitudinal centre of gravity (CG) range, necessitating a larger HTP to maintain longitudinal stability and control authority.

In the aircraft industry, manufacturers commonly develop families of aircraft based on a shared platform. An aircraft family consists of products that share key components and processes while allowing each variant to meet specific operational requirements [7]. Typically, there is a base model which serves as the reference, with other variants derived from it [8]. Families enable different combinations of range and payload with minimal modifications to the base design. The most common design strategy maintains constant fuel capacity to preserve wing commonality, achieving a trade-off between payload and range by stretching or shortening the fuselage, as exemplified by the Airbus A320 family. Other approaches involve creating extended-range (ER) variants by increasing fuel capacity. These variants can also carry higher payloads compared to the base family member, as illustrated by the Boeing 777 family, where the 777-200 serves as the reference model [9]. The empennage size is strongly affected by family design. Changes in fuselage length alter the horizontal and vertical tailplanes (HTP and VTP) lever arms, requiring adjustments in sizing to meet stability, trim, and control requirements [10]. While tailored tailplanes are ideal, manufacturers often share the same tail across family members to maximize commonality, resulting in oversized surfaces and a trade-off between performance and commonality. This approach has proven feasible in conventional aircraft families such as the A320 [11–13] and Airbus A350 [14].

Although empennage commonality is well established in conventional kerosene-powered aircraft families, existing studies on LH2 aircraft have largely focused on individual point designs. To the authors' knowledge, no prior work has systematically investigated family-level commonality for hydrogen-powered aircraft. While a limited number of studies address LH2 aircraft family design [15, 16], they do not explicitly examine the degree of component commonality across the family. Consequently, it remains unclear whether a shared empennage, as used in conventional families, is feasible for LH2 configurations, particularly in light of the stability and control challenges introduced by rear-fuselage hydrogen storage. To address this limitation, the study formulates a set of research questions, all evaluated using the block fuel penalty of a family design relative to its corresponding point-optimized configuration as the primary performance metric. First, what is an acceptable performance penalty, in terms of block fuel, for a conventional kerosene-powered aircraft family compared to its optimized point design? Second, how does this penalty compare to that of an LH2 aircraft family using a traditional shared-tank design approach? Finally, how does the penalty evolve when the degree of commonality is reduced, allowing for variations in tank size across family members? By addressing these questions, the study systematically evaluates the performance–commonality trade-offs associated with shared empennage design in LH2 aircraft families.

The document is structured in the following way: Section 2 explains the methodology developed to conduct the aircraft designs studies. It details a simultaneous design methodology that mirrors industry practice by sizing all family members concurrently, ensuring each variant's design influences the others [8]. Section 3 defines the reference, baseline, and LH2 aircraft concepts used as the starting point. These are based on the existing aircraft concepts within the German Aerospace Center (DLR) EXACT project [17]. Section 4 outlines the calibration and verification procedures followed, using publicly available data. In Section 5, the results are presented for the different family design studies and trade-offs conducted. Lastly, Section 6 summarizes the general trends and guidelines resulting from the design space exploration, that can be applied for the design of LH2 aircraft families with rear-fuselage tanks.

2 Design methodology

A DLR in-house conceptual aircraft design workflow has been modified to address the objectives of the paper. The baseline methodology was originally developed within the DLR EXACT project, where it was applied to conduct multiple trade-off studies and to generate several LH2 aircraft design concepts ([4, 18, 19]). A schematic of the workflow is shown in Fig. 1. The framework is supported by the Common Parametric Aircraft Configurations Schema (CPACS), facilitating data exchange between tools; and the Remote Component Environment (RCE) software, used to link the different tools. The tools coupled, represented by squares in Fig. 1, include two different levels of fidelity.

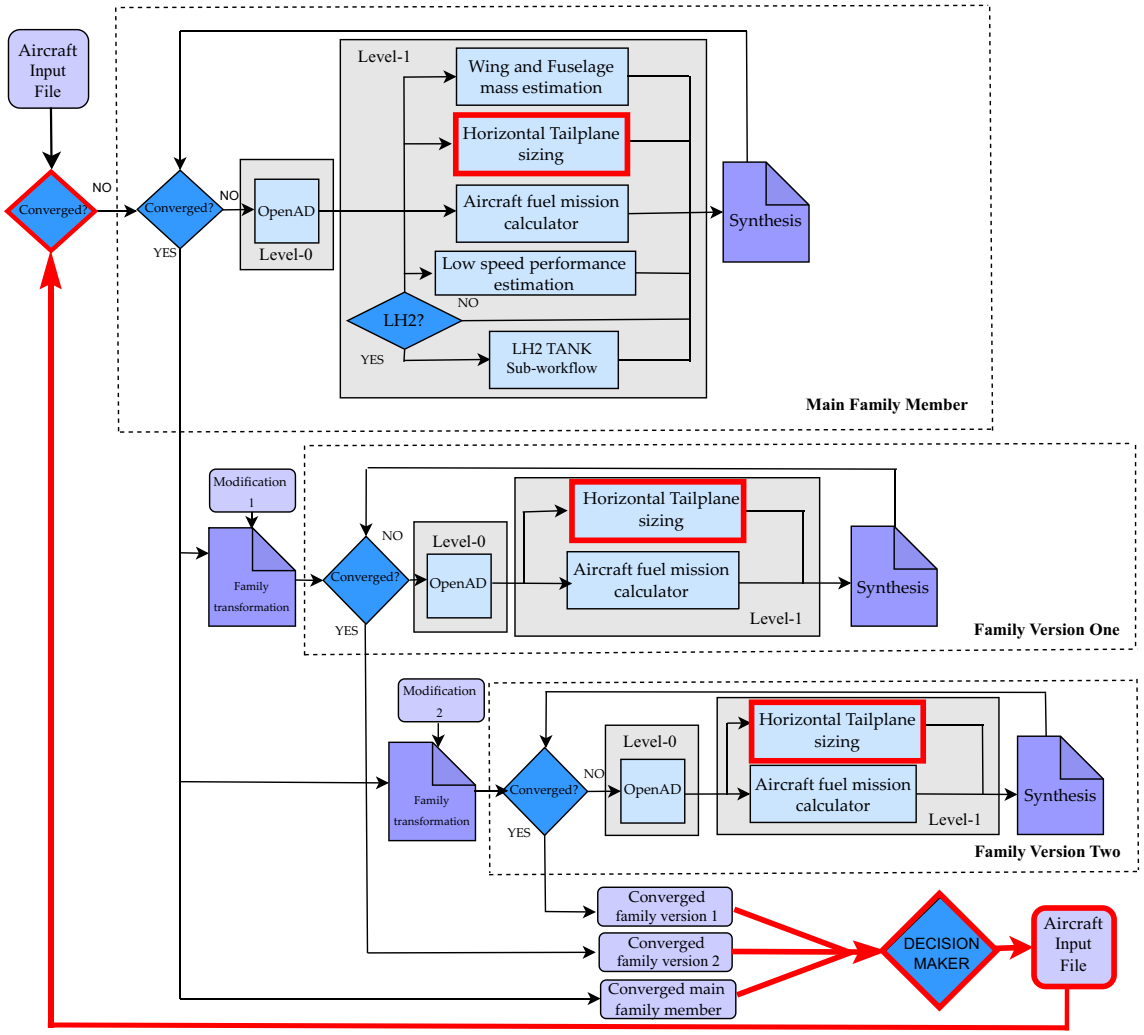


Fig. 1 Modified EXACT workflow schematic

- Level-0 methodologies: based on handbook methods, mainly statistical or empirical expressions. They allow for the exploration of the design space at a low computational cost [20]. This is the case for openAD, which is the in-house DLR overall aircraft design software [21]. It mainly determines the initial aircraft geometry, mass- and aerodynamic breakdown. It creates engine decks as well based on a simplified engine thermodynamic cycle calcualtion with constant component efficencies.
- The rest of the tools can be classified as Level-1 fidelity methodologies. Each of them focuses on a specific discipline within overall aircraft design. The methods inside them are more complex, and based on simplified physics models, that are applicable to simple extensions of the design space [22]. These are the aircraft fuel mission calculator tool [4], the low speed performance tool [23], the hydrogen tank sizing routine (from [24]), and methodologies for the estimation of the fuselage and wing structural masses [25–28].

As depicted in Fig. 1, the workflow is composed of three convergence loops or sub-workflows. Each of them corresponds to a family member. For each aircraft, the design process begins with openAD, which defines a preliminary aircraft configuration. This initial design is then refined using the Level-1 fidelity tools that recalculate key parameters for the different disciplines. In the next iteration, openAD receives new inputs based on the Level-1 tool results through the "Synthesis" script, resulting in a refined design. The process is repeated until convergence. The "main" family member is designed first. Then, the results of the design are passed to the family "versions" 1 and 2. Here, the "Family transformation" scripts are introduced, which are used to define the family "versions" based on the "main" family member output. The "versions" 1 and 2 are defined based on the change in total fuselage length (Δl_f), the change in fuselage length due to sections placed behind the wing (Δl_{VTP}), the change in mass per meter of cabin section ($\frac{dm_f}{dl_f}$, where m_f represents the fuselage mass), and the change in payload-range

capability, with respect to the "main" family member. At the same time, the "family scripts" ensure that certain constraints for aircraft family design are met. For instance, having the same relative position of the main landing gear to the wing chord (ξ_{mg}), or having a feasible wing root position along the fuselage length ($x_{root,LE}$) based on a fixed length for the fuselage family sections. The expressions applied to go from the "main" member to the "family versions" can be found below:

$$\text{length of the fuselage} : l_{f_{version}} = l_{f_{main}} + \Delta l_f \tag{1}$$

$$\text{mass of the fuselage} : m_{f_{version}} = m_{f_{main}} + \frac{dm_f}{dl_f} \cdot \Delta l_f \tag{2}$$

$$\text{main landing gear position} : \xi_{mg_{version}} = \xi_{mg_{main}} \tag{3}$$

$$\text{wing root position} : x_{root,LE_{non-sizing}} = x_{root,LE_{sizing}} + \Delta l_f - \Delta l_{VTP} \tag{4}$$

The meaning of the subscripts "sizing" and "non-sizing" in expression (4) are explained further down in Sect. 2.2. The components highlighted in red in Fig. 1, constitute the modifications done to the EXACT workflow with respect to the base methodology. The improved version is able to systematically size an aircraft, with special emphasis on its tailplane, considering not only the given Top Level Aircraft Requirements (TLARs), but also potential family members. Two main changes were implemented, explained in the following sections.

2.1 Horizontal tailplane sizing tool

Special emphasis is placed on the sizing process of the HTP, as mentioned in the introduction. A new Level-1 fidelity tool based on the scissors plot methodology [10, 29] is implemented into the workflow. The methodology is based on the analysis of the moment equilibrium of the aircraft among different flight phases. This more detailed assessment allows to model the main differences between kerosene and LH2 aircraft regarding the mass distribution along the longitudinal axis. The original semi-empirical and statistical methods available in openAD are still used to size the vertical tailplane (VTP).

The so-called X-plot or scissors plot, is a graph that represents the required area ratio of the HTP to the wing (S_h/S) as a function of the longitudinal CG range, commonly shown as a percentage of the length of the mean aerodynamic chord (MAC) (x_{cg}/MAC). Multiple lines are plotted, each representing a specific sizing requirement for the HTP and indicating the necessary tailplane area for a given CG position along the MAC under a particular flight condition. The equations defining these lines are based on different HTP sizing criteria. In this study, three criteria are considered: take-off rotation, controllability (trim), and stability. A brief description of each is provided below:

- *Controllability requirement (trim)*: the HTP has to be able to generate a moment in a way that ensures a longitudinal equilibrium of all forces, that in the end, results in a moment equal to zero around the aircraft CG. At this point, the aircraft is said to be trimmed [10]. When moments are evaluated about the aircraft CG, the resulting expression may be rearranged into a linear form (see (5)). This formulation, which parallels the derivation in [29], allows the controllability boundaries to be mapped directly onto the scissor plot:

$$\frac{S_h}{S} = A \cdot \frac{x_{cg}}{MAC} + B \tag{5}$$

The A and B coefficients depend on the aircraft geometry (such as the horizontal tailplane lever arm and aerodynamic centre positions), as well as on the engine characteristics and overall aerodynamics [10, 29]. The coefficients vary with the flight condition and flap setting, with the most critical trimming scenario typically occurring in the landing configuration, which imposes a limit on the most forward in-flight CG position of the aircraft [10]. This implies that the farther forward the CG is located, the larger the horizontal tailplane (HTP) must be to satisfy the trimming requirement.

- *Stability requirement*: the aircraft has to be longitudinally statically stable for all its CG positions. This means that the derivative of the pitching moment coefficient with respect to the angle of attack has to be negative [10]. This condition can be re-arranged also as a linear equation like (5), giving the required HTP area (S_h/S) as a function of the CG position (x_{cg}/MAC). In this case, it is the cruise condition the one that usually represents the sizing case for the HTP from a stability point of view, limiting the most aft in-flight CG [10, 29].
- *Take-off (TO) rotation requirement*: the HTP is not only responsible for trimming the aircraft and ensuring stability, but also for providing sufficient control through the elevator during certain manoeuvres. Take-off is especially relevant, as the HTP has to be able to provide enough lift to rotate the aircraft around the main landing gear at an acceptable angular acceleration [10, 30]. Considering all forces and moments acting on the aircraft during rolling, a third expression can be deducted that can also be rearranged in the form of a linear equation. The model used for this requirement is taken from [30]. The requirement can be analysed for different aircraft weight configurations, being often the most critical the one with the most forward CG. This latter requirement

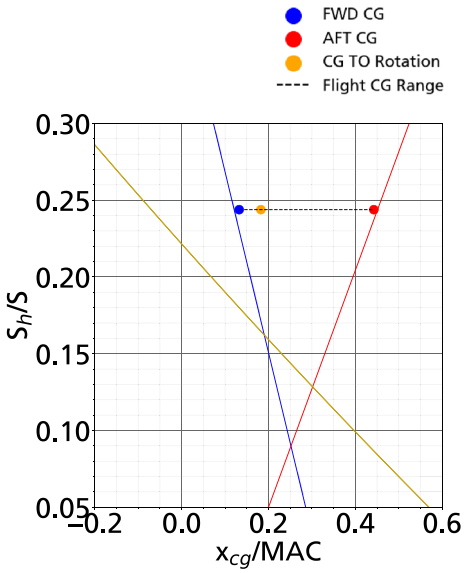


Fig. 2 Example of minimum HTP area for trim and stability

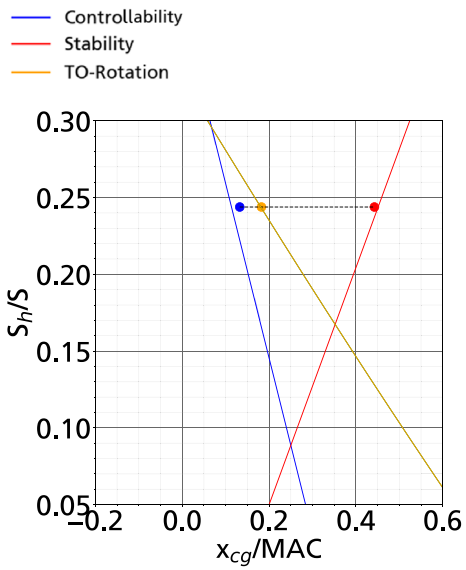


Fig. 3 Example of minimum HTP area for stability and TO rotation

then imposes a limit for the most forward CG of the aircraft, in this case for ground operations. For the study, it is expected to be slightly behind the most forward in-flight CG (5% of MAC behind), as indicated in some available commercial aircraft data [31].

The equations for each HTP sizing requirement include multiple aircraft geometric, aerodynamic, and engine performance parameters. In case these are not given in the CPACS data structure, they are estimated using semi-empirical methods taken mainly from the USAF-DATCOM [32]. The first two requirements are analysed along the discretized flight envelope boundary for clean, take-off, and landing configuration. The take-off rotation is analysed for different take-off masses. Only three lines are shown in the final plot, the most limiting ones, one for each requirement. The CG range is plotted, including the most forward and aft in-flight CG positions, and most forward on-ground CG position. The lines define a region with the shape of a scissor, where the CG range has to be contained. Therefore, the minimum HTP area is found when the range lies perfectly between two of the boundaries. Examples of the two possible solutions are shown below in Figs. 2 and 3.

A link is implemented between openAD and the HTP sizing tool through the synthesis script (see Fig. 1) to find the minimum HTP solution. The wing longitudinal position is iteratively changed. After each iteration, the scissor plot is analysed.

1. If the HTP area is smaller/bigger than it should be, the size is adjusted.
2. The relative position of the CG range to the boundaries of the scissors is studied. The wing position is adjusted accordingly.

    - If the wing is too far aft, the situation is identified in the plot with the most aft CG being far in front of the stability limit. The control requirement (or take-off rotation requirement) is oversizing the HTP, being the most forward CG for in-flight operations (or on-ground) over the controllability boundary (or take-off rotation boundary). The wing can be shifted forward, resulting in a more optimal wing position and thus smaller HTP.
    - If the wing is too far in front the opposite case is given. Both most forward centers of gravity for in-flight and on-ground operations are positioned behind the controllability and take-of rotations limits respectively, with the stability requirement acting as the constraint for the HTP area. To reduce the required area, the wing can be shifted backwards.

    The methodology identifies which case applies, and corrects the wing position.

3. The new HTP area and wing longitudinal position are fed back to openAD through the synthesis script. The values are fixed for the next iteration of the design, repeating the process until the design has converged, resulting in the minimum HTP area. Two possible outcomes exist for the routine, depicted in Figs. 2 and 3, for an aircraft whose in-flight CG spans from 15% (20% for TO) to 45% of the MAC. Both cases result in an $S_h/S = 0.245$.

- *Minimum HTP for trim and stability*: the in-flight CG lies perfectly between the control and stability requirements. All requirements are meet. The tail is slightly oversized for take-off rotation, as the CG for rotation lies behind its limit (orange line). Adjusting the wing position to solve this worsens the other requirements. Figure 2 shows an example.
- *Minimum HTP for stability and take-off rotation*: the most forward CG for on-ground operations (TO) lies now perfectly over the take-off rotation limit. It is represented in Fig. 3. The tail is now oversized for the controllability requirement, since the most forward CG is slightly behind the blue line. Shifting the wing, leads to a sub-optimal result regarding the stability boundary.

2.2 Outer-Family convergence loop

The second addition to the workflow consists of an outer loop that feeds information gathered from all family members back into the main family design. Initially, the main aircraft was sized independently, determining the required VTP and HTP areas for the design. Then, the information was passed and fixed as an input for the family versions. Thus, it was always considered that the main family version was sizing for both the HTP and VTP. The workflow can now assess whether any of the family versions requires a larger tailplane, influencing the design of the main family member. The sizing routine is divided into two parts now:

- *Point design phase*: firstly, all aircraft are sized independently. The required sizes for both the HTP and VTP are determined, along with the optimal wing position. At this stage, the wing can be positioned freely along the longitudinal axis, without considering family design constraints. Thus, expression (4) is not used. At the end of this phase, the results for the HTP and VTP sizes across all aircraft are evaluated in the decision-making block, which identifies the most critical variant.
- *Family design phase*: once the sizing aircraft for both the HTP and VTP is identified, the corresponding empennage sizes are fixed and imposed on the other two variants. The aircraft design loops are reiterated for all aircraft, this time incorporating the common empennage into each design. The wing position of the "non-sizing" aircraft is readjusted in this phase. During the point design phase, the wing location was unconstrained. However, in practice, when designing a family of aircraft, the wing position cannot be arbitrarily defined. It must be coordinated across all family members, taking into account the overall change in fuselage length (Δl_f) and the change in fuselage length due to added or removed fuselage sections behind the wing (Δl_{VTP}), as illustrated in Fig. 4. The final wing position of the "non-sizing" variants is selected so that, after adjusting the fuselage length, the resulting wing location for the "sizing" variant aligns with the optimal position for minimum HTP area. This is done with expression (4).

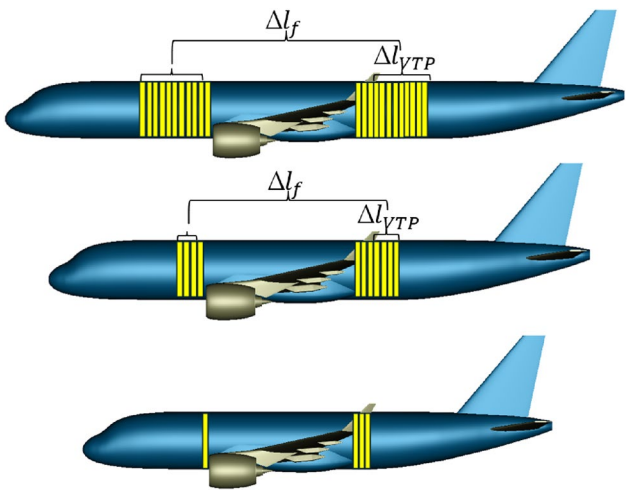


Fig. 4 Example of the change in fuselage length and wing position for an aircraft family

The point design executes each aircraft design loop only once. However, the family design phase might need a few more iterations of the outer loop to converge, recalculating each aircraft design loop multiple times. This is because the main aircraft design is linked to the family versions as depicted in Fig. 1. Changing the main design impacts the family versions, and as a result the critical HTP and VTP sizes for the family. Thus, once the sizing aircraft is identified, the empennage and wing position of the remaining members are adjusted until achieving a converged family with a common tail size. The HTP and VTP sizes are converged in parallel.

The calculation method for the VTP size is comparatively simple. An empirical formulation is implemented in openAD to estimate the vertical tail volume coefficient based on key aircraft geometric parameters, including the fuselage length. The equation used is considered sufficient for the purpose of the study to account for the variations in VTP size among the different family members due to its consideration of the difference in fuselage length.

Each aircraft design sub-workflow runs all disciplinary tools in parallel. After each iteration, the OEM (operating empty mass) and MTOM (maximum take-off mass) values are evaluated to check for convergence. In contrast, the outer family loop monitors the HTP and VTP surface areas at the end of each iteration. To ensure consistent convergence criteria, the tolerances for the inner-aircraft design loops are set such that a mass difference (in kg) corresponds

to an acceptable surface area difference (in m^2) for the convergence of the outer-family loop. For this study specifically, a difference of 0.5 m^2 was considered for a converged empennage size.

Note that the methodology described is applicable only when the stretched variant serves as the main family member. The "Family transformation" scripts adjust component positions and centers of gravity based on the change in fuselage length of each variant relative to the main design. During the point design phase, only the HTP and VTP are resized for each aircraft; all other components, such as the engines and landing gear, are sized based on the main design and remain fixed for the other variants. Since these components are typically driven by the requirements of the largest family member, only that variant is suitable to serve as the base or main design. This ensures that all shared components, and not only the empennage, are sized for the most demanding variant.

3 Aircraft concepts for the study

In this section the concepts used for this study are presented. All aircraft are existing concepts derived from the DLR EXACT project. Their design has been refined due to the enhanced methodology for HTP sizing.

3.1 Reference aircraft: the DLR D239 concept

The reference aircraft is used as the basis to calibrate the methodology applied during the aircraft design study, serving at the same time as a model for comparison and sensitivity studies. The reference chosen is the DLR D239 aircraft concept, shown in Fig. 5. It resembles the DLR interpretation of an aircraft similar to the Airbus A321neo with technology factors from 2016, based on publicly available data [11–13]. It was used for the EXACT project short-medium-range class concepts [18]. The TLARs are summarized in Table 1 (TOFL stands for Take-Off Field Length).

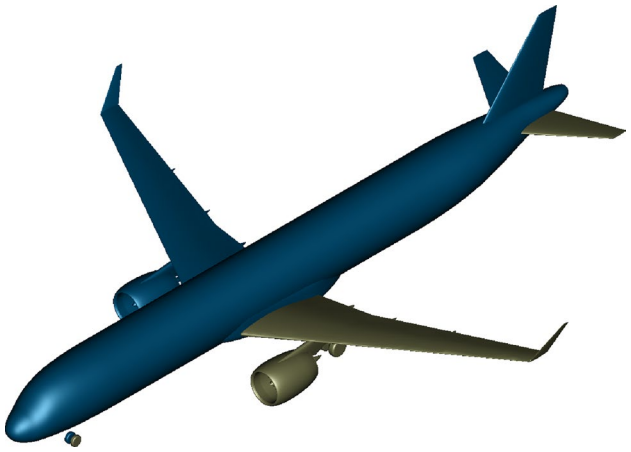


Fig. 5 D239 ISO-view

Table 1 D239 reference aircraft concept TLARs [18]

TLAR	Value	Units
Design Range	2500	NM
Design PAX (single class)	239	-
Mass per PAX	95	kg
Design Payload	25000	kg
Max. Payload	25000	kg
Cruise Mach number	0.78	-
Max. operating Mach number	0.80	-
Max. operating altitude	40000	ft
Approach speed	136	kt
TOFL (ISA +0K SL)	2200	m
Rate of Climb @ TOC	>300	ft/min
Wing span limit	≤ 36	m

Table 2 D250 baseline aircraft concept TLARs [18]

TLAR	Value	Units
Design Range	1500	NM
Design PAX (single class)	250	-
Mass per PAX	95	kg
Design Payload	23750	kg
Max. Payload	25000	kg
Approach speed	140	kt
TOFL (ISA +0K SL)	1900	m
Wing span limit	≤ 42	m

3.2 Baseline aircraft: DLR D250 concept

The concept of baseline aircraft is also widely used in the overall aircraft design context. It represents an evolved version of the reference aircraft. Technology factors are applied that account for aircraft performance improvements in different disciplines. This configuration serves as a conventional baseline, assuming an Entry into Service (EIS) concurrent with the technologies under investigation. As its name indicates, the baseline is used as a base for the development of new aircraft concepts and to compare the obtained results. The D250 kerosene aircraft concept is a short-medium range (SMR) turbofan powered aircraft. It was developed as the baseline model for the EXACT LH2 concepts [18]. The TLARs are summarized in Table 2. The TLARs are derived from the D239 baseline, with the main modifications being an updated range and payload to ensure comparability between the D250 kerosene configuration and an LH2 concept [18], as well as an increased wingspan limit reflecting a higher aspect ratio wing. The aircraft is powered by an incrementally improved version of the geared turbofan employed on the D239. Furthermore, technology factors have been applied across the various disciplines to reflect the EIS of 2040. A summary of these modifications is

Table 3 D250 baseline technology factors compared to the D239 reference [18]

Parameter	Technology Factor
BPR	+ 15% from Reference (BPR = 12)
OPR	+ 25 % from Reference (OPR = 36)
Gas Turbine	+ 5% efficiency and no thrust reverse
Fuselage	– 5% mass vs. state of the art
Wing	CFRP wing with foldable wingtips
Empennage	– 8% mass

Table 4 Family versions definition for the D239 family concept

TLAR	D239	D239-mid	D239-short	Units
Design Range	2500	2900	3300	NM
Design PAX (sing. class)	239	185	156	-
Design Payload	25000	17000	16400	kg
Max. Payload	25000	19200	19000	kg
Δl_f	0	− 6.93	− 10.67	m
Δl_{VTP}	0	− 2.70	− 4.70	m
dm_f/dl_f	-	275	275	kg/m

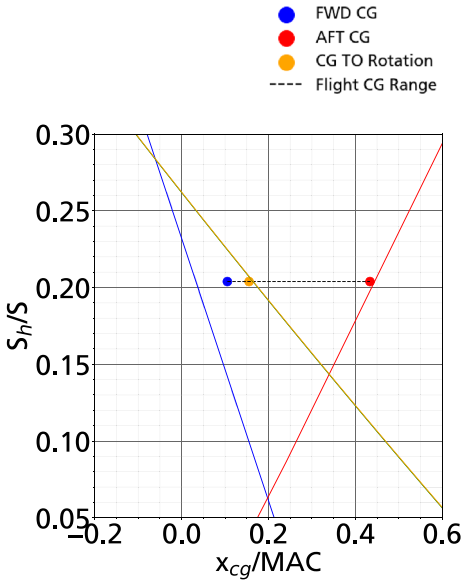


Fig. 6 D239 (Point design) scissors

presented in Table 3 (where CFRP stands for Carbon Fiber Reinforced Polymer).

3.3 LH2 aircraft: D250-LH2 concept

The D250-LH2 concept was developed from the D250 baseline, and represents a SMR aircraft with two turbofan engines powered by direct combustion of liquid hydrogen. The TLARs of this concept are the same as shown in Table 2 for the D250 kerosene baseline. The concept is also part of the results of the EXACT project. It incorporates two cryogenic non-integral hydrogen tanks for redundancy, located behind the cabin at the unpressurized rear of the fuselage.

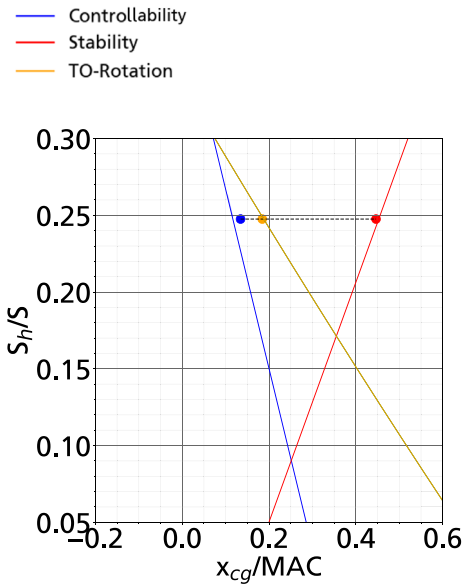


Fig. 7 D239-S (Point design) scissors

The tanks are made from aluminium, and insulated using multi-layer insulation (MLI) [19]. Note that the concept presented in [19] featured a conventional horizontal tail configuration, as also does the kerosene D250 baseline. However, in more recent updates of the concept, this configuration has evolved into a T-tail. It ensures a better integration solution for the cryogenic tanks, while also decreases the required HTP area.

4 Calibration

This section showcases the calibration and heuristic validation procedure and results of the enhanced EXACT workflow. The D239 reference aircraft (see Figure 5) is used as the calibration case, and is sized as the main family member. Two shorter versions are derived from it. These are interpretations similar to the A320neo and A319neo aircraft, and named for this study D239-mid and D239-short respectively. The three aircraft constitute the D239 family. The definition of the two shorter family versions is done based on a series of parameters used in the "Family transformation" scripts, as explained in Section 2 of the document. Their values are shown in Table 4.

Each family member, D239 (L), D239-mid (M) and D239-short (S) is designed independently first to reach the design points specified in Table 4. The empennage is sized for minimum area. Once the sizing member for the empennage is identified, the tailplane tools requirements are manually calibrated to fit the CG range of the sizing family member. Lastly, all family variants are redesigned until a common empennage size is found. The HTP sizing process

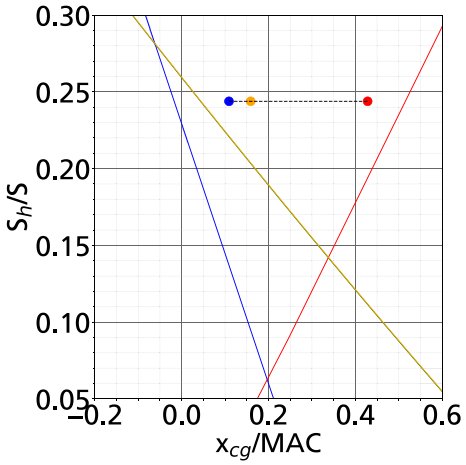


Fig. 8 D239 (Family design) scissors

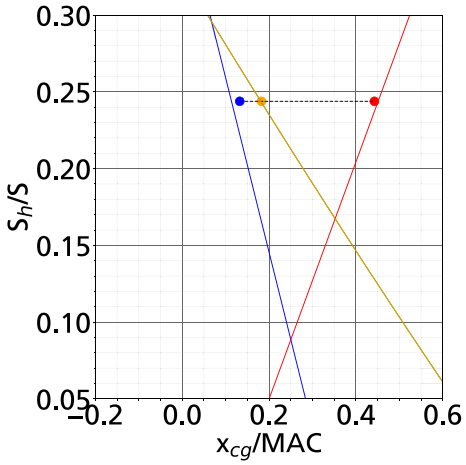


Fig. 9 D239-S (Family design) scissors

can be seen in the scissor plots shown in Figures 6-7 and 8-9. The first two illustrate the point designs, and the last two the family designs of both D239 and D239-short.

Starting with the point design, the HTP area is constrained for both aircraft by take-off rotation and stability requirements, similar to the example in Fig. 3. The aircraft's CG range, which is estimated by using 6 different combinations of design masses, payload and fuel, must remain within the region defined above the intersection of the red and orange lines. The trim (or controllability) requirement (blue) does not limit the HTP area. In both plots, the CG range lies perfectly within the bounds set by the take-off rotation and stability constraints, indicating that the HTP area has been minimized and tailored for each point design. The CG range is similar for both aircraft. However, the shorter lever arm of the -short variant is reflected in the scissor plot as a narrower feasible region, ultimately resulting in a larger S_h/S value. Note that in both cases, the wing reference area is assumed to be 129 m^2.

For the final D239 family design, the HTP is oversized for the long-fuselage variant (compare Figs. 6 and 8), as indicated by the CG range lying well within the scissor plot boundaries with a noticeable margin relative to the point design. A similar trend is observed for the D239-mid final family design. Consequently, the HTP area is dictated by the short variant and subsequently applied across the family, while the short variant itself remains largely unchanged between the point and family designs. These trends can only be partially assessed through consistency with established aircraft design principles, as no publicly available data exists regarding the actual sizing aircraft within the D239 similar A320 family or the corresponding point-design tailplane areas of the remaining variants. Identifying the D239-short as the sizing family member is consistent with the expected trend resulting from its shorter tail moment arm. Based on this assumption, the employed methodology was calibrated to reproduce the publicly available HTP area of the overall family design [11–13]. The resulting tailplane surface area predictions for the D239-M and D239 variants follow the expected physical trend, although a direct quantitative validation is not possible due to the lack of publicly available reference data. Additional qualitative support for these findings can be drawn from an incident report published by the Air Accidents Investigation Branch (AAIB) concerning an Airbus A321 [33]. The report suggests that the aircraft possesses a comparatively oversized tailplane and reaches its forward CG limit through take-off rotation constraints rather than controllability limitations. Despite operating at an excessively forward CG position outside of the operational range, the aircraft remained controllable but barely achieved sufficient rotation for lift-off. Both tendencies are predicted for the D239 family design (see Fig. 8). Appendix A provides three-view drawings of the final D239 and D239-short designs.

The results for all family members in the initial design loop (point design) and the final family design are summarized in Table 5. Both the horizontal and vertical tailplanes are sized by the short-fuselage variant, which features the smallest tail moment arm. The table presents the variations in key geometric parameters, including empennage areas (S_v and S_h) and wing position ($x_{root,LE}$), for both point and family designs, and links these changes to their impact on operating empty mass (OEM) and maximum take-off mass (MTOM). Ultimately, these geometric and mass variations translate into differences in mission fuel mass (MFM), which is used to quantify the block fuel penalty associated with adopting a family design relative to the optimized point designs.

As observed, the largest penalty occurs for the long-fuselage variant, as its optimal empennage size deviates most from the common family configuration. Overall, adopting

Table 5 Comparison of the D239 aircraft variants point and family designs

	Point design			Family design		
	L	M	S	L	M	S
$x_{root,LE}$ [m]	16.68	12.68	10.85	16.77	12.54	10.85
S_v [m^2]	18.07	19.19	20.50	19.92	19.92	20.06
S_h [m^2]	26.20	29.28	31.81	31.45	31.45	31.19
Payload [kg]	25000	19000	16400	25000	19000	16400
OEM [kg]	50029	43806	42010	50378 (+0.7%)	44055 (+0.57%)	42164 (+0.37%)
MTOM [kg]	92717	79576	75889	93350 (+0.68%)	79948 (+0.47%)	76073 (+0.24%)
MFM [kg]	17688	16872	17581	17972 (+1.6%)	16997 (+0.74%)	17613 (+0.18%)

Table 6 A320neo family data [11–13]

	A320 neo family		
	A321 (L)	A320 (M)	A319 (S)
$x_{root,LE}$ [m]	16.80	12.71	10.86
S_v [m^2]	20.4	20.4	20.4
S_h [m^2]	31.0	31.0	31.0

a family design for the D239 (L) increases the OEM by approximately 0.7%, primarily due to the larger empennage required by the short variant. This increase propagates through the design in a compounding manner: heavier tail surfaces require larger engines, which in turn drive increases in wing and fuselage structural weight. As a result, a mission fuel mass penalty of approximately 1.6% is observed for a 2500 NM mission. This level of penalty is consistent with industry practice and is generally considered an acceptable trade-off given the benefits of component commonality. The members of the Airbus A320neo family share a common empennage configuration [11–13]. The results therefore provide a useful reference point for benchmarking the performance impact of commonality in kerosene-powered aircraft families, which can subsequently be compared to LH2 configurations.

The wing position, during the point design phase it is optimized independently for each aircraft to minimize empennage size. However, in the final family design, the wing position of the non-critical members deviates from these individual optimum (see Table 5), as it is readjusted to satisfy the family design constraints defined in Table 4, following Equation (4). For the D239-short variant, which acts as the sizing member, both the tailplane areas and wing position differ slightly from those obtained in the point design iteration. These variations propagate to small changes in OEM, MTOM, and MFM. This discrepancy is caused by the iterative coupling within the family design process, whereby modifications to the main family member influence the subsequent sizing of the -short variant. A minor difference also remains between the horizontal and vertical tailplane areas of the D239-short and those of the other family members. However, this difference is below the convergence tolerance of 0.5 m^2 defined for the outer loop. The family design can therefore be considered converged to a common empennage area.

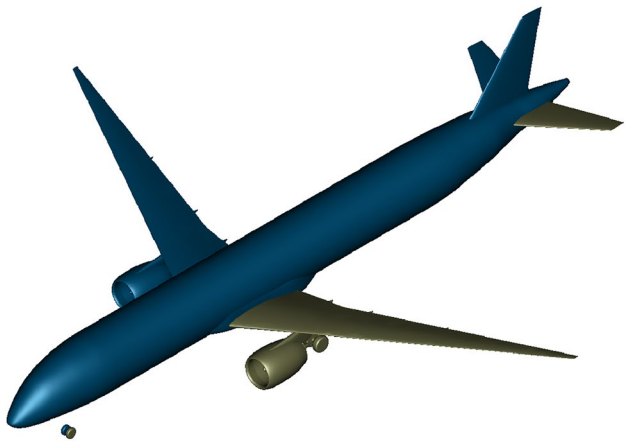


Fig. 10 D250 main family member (long version) ISO-view

The final results for the reference D239 aircraft family shown in Table 5 can now be compared to the publicly available data for the A320neo family [11–13]. The main parameters are summarized in Table 6. The values for the reference closely align with the numbers in the table below.

5 Results and discussion

This chapter provides a comprehensive evaluation of the results obtained across the different aircraft family conceptual design studies. The present work is based on the methodology and findings of the DLR EXACT project, utilizing both the D250 baseline [18] and D250-LH2 [19] concepts to conduct the various studies. Both concepts are represented in Figs. 10 and 11 respectively.

First, both concepts are redesigned using the enhanced aircraft sizing workflow. The improvements introduced in Chapter 2 enable trade-off analyses that were not possible during the initial design phase. Following this, aircraft families are derived from both the D250 and D250-LH2 concepts, following the same strategy applied to the D239 reference family. In each case, two shorter variants are generated, with their corresponding definitions provided

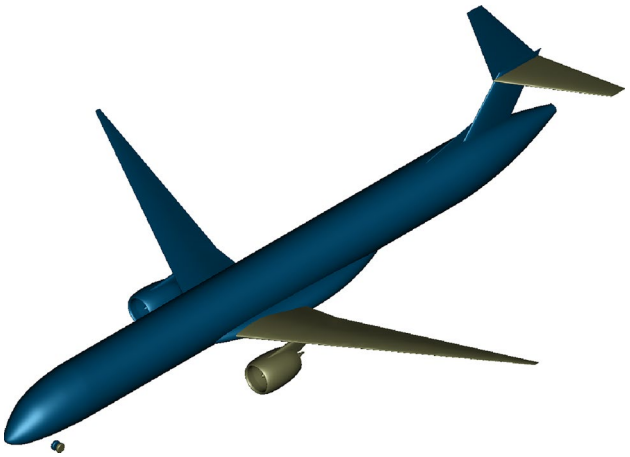


Fig. 11 D250-LH2 main family member (long version) ISO-view

Table 7 Family versions definition for the D250 and D250-LH2 family concepts

TLAR	D250/D250-LH2	D250-mid	D250-short	Units
Design Range	1500	1700	2000	NM
Design PAX (sing. class)	250	220	190	–
Design Payload	23750	20090	18050	kg
Max. Payload	25000	22000	19000	kg
Δl_f	0	− 3.7	− 7.4	m
Δl_{VTP}	0	− 1.85	− 3.7	m
dm_f/dl_f	-	305	305	kg/m

in Table 7. The range of the shorter variants is determined based on the main D250 family member, using a proportional scaling consistent with that applied to the D239 family. Similarly, the passenger capacity of the shorter variants is defined using the same passenger ratio adopted for the reference aircraft family.

In the final section of the chapter, the sensitivities of the D250-LH2 family design are further examined.

5.1 Landing gear integration trade-off study

The modifications done to the workflow led to new design trade-offs for both the D250 and D250-LH2 configurations. A significant trade-off emerging is between wing-mounted and body-mounted landing gear. The D250 concept features a shorter inner wing chord. The optimization of the horizontal tailplane area, achieved by the implemented algorithm through a shift of the wing, results in a wing position that prevents integration of the landing gear within the wing structure. Shifting the wing forward causes the aircraft's CG range to move aft relative to the wing chord, which

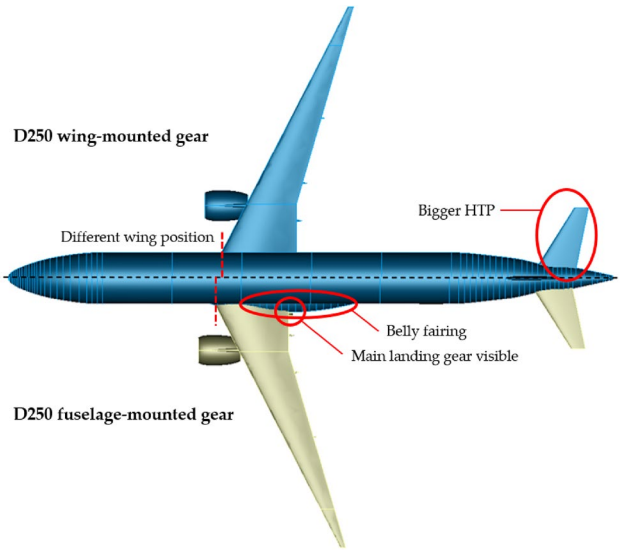


Fig. 12 Plan view of the D250 concept (point design) with fuselage-mounted (bottom) and wing-mounted landing gear (top)

in turn displaces the landing gear location rearward. This leads to a point where the wing is positioned so far forward that wing mounted landing gear integration becomes unfeasible. Thus, the D250 design requires a trade-off between fuselage-mounted and wing-mounted landing gear, which affects its final wing position and HTP area. The main geometric differences between both concepts are depicted in Fig. 12, which presents both possible D250 point designs. Under the symmetry line, the fuselage-mounted solution is shown, featuring a belly fairing. Above the symmetry line, the wing-integrated concept is depicted, displaying a slightly aft wing position.

The landing gear integration trade-off is even more critical for LH2 aircraft with rear-mounted tanks. Due to the larger CG range, the main landing gear must be positioned further aft to ensure ground stability. In a wing-mounted landing gear configuration, this requirement can drive the wing position significantly rearwards, leading to a non-optimal HTP area. A potential mitigation strategy is to reduce the allowable operational CG range [4]. Since the landing gear position is determined by the most aft CG condition, which for LH2 aircraft with rear tanks typically corresponds to ferry flight conditions, operational constraints can be introduced to limit aft CG excursions. For instance, enforcing a minimum payload requirement can restrict the aft CG shift, enabling a more forward landing gear position and, consequently, a more favourable wing placement and HTP sizing. For LH2 aircraft, this approach implies a reduction in maximum fuel load during ferry or low-payload missions, effectively decreasing the achievable ferry range. The nominal range can still be maintained when sufficient payload is carried. Additionally, the use of a tail stand may be required

during refuelling of an empty aircraft to full tank capacity. However, these measures reduce the overall flexibility of both the aircraft design and its operational envelope [4].

The effect of the landing gear integration trade-off on the scissor plot can be observed in Figs. 13 and 14 for the D250 main family member. The same behaviour is found for the shorter variants as well as for the LH2 configurations. For the wing-integrated solution (see Fig. 14), the relative position of the main landing gear along the wing chord (ξ_{mg}) is constrained. Its value is fixed to $\xi_{mg} = 0.8$, leaving the aft 20% of the wing chord available for high-lift device mechanisms. This constraint introduces an additional limitation in the scissor plot, effectively restricting the allowable aft centre-of-gravity (CG) position, as illustrated in Fig. 14. Although the aft CG limit remains ahead of the stability boundary, further forward wing movement without modifying the landing gear integration becomes unfeasible. This results in a sub-optimal wing position and, consequently, an oversized horizontal tailplane. Once this constraint is reached, the wing cannot be shifted further forward.

At first glance, the HTP areas for both configurations appear similar, as shown in Figs. 13 and 14, which may seem counter-intuitive. However, this is a coincidental result arising from differences in mass distribution between the configurations. When considering all family members, the overall trend supports the initial hypothesis: configurations with fuselage-integrated landing gear generally require smaller horizontal tailplane areas across the family (see also the LH2 designs shown in Table 8).

Table 8 presents the results of the landing gear integration trade-off. The D250 configuration is evaluated with both wing-mounted and fuselage-mounted landing gear. The D250-LH2 concept is assessed under the same configurations, additionally considering both full and reduced CG range cases to constrain aircraft operations. For the reduced CG range variant, no specific regulatory limitations were identified. A shift of the aft CG limit forward by 0.4 m (10 % MAC) was considered a reasonable compromise between performance and operational flexibility, effectively reducing the CG range by 15%. The minimum payload without operational constraints at maximum tank capacity is 28 %, which is well below an average or profitable capacity factor and thus would rarely occur in regular airline operations

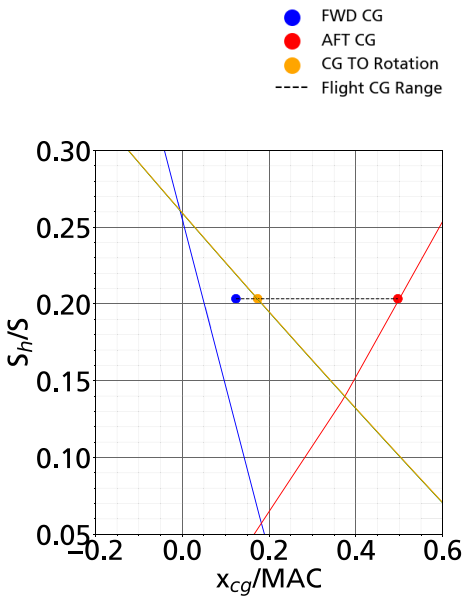


Fig. 13 Scissors plot for the D250 with fuselage integrated landing gear (Point design)

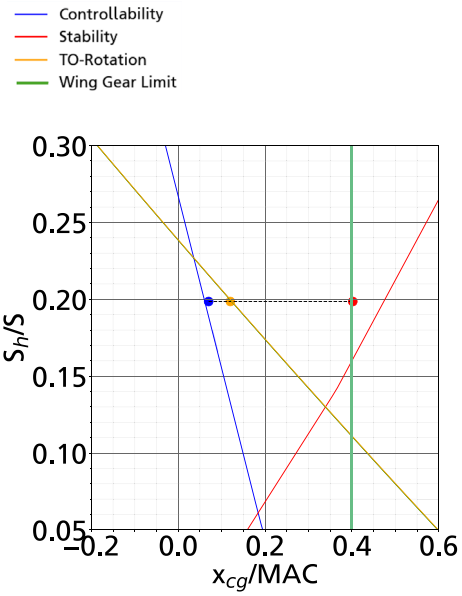


Fig. 14 Scissors plot for the D250 with wing integrated landing gear (Point design)

Table 8 Impact of landing gear integration on geometry and performance of the D250 and D250-LH2 point designs

	Wing-Mounted			Fuselage-Mounted		
	D250	D250-LH2 (red. CG)	D250-LH2	D250	D250-LH2 (red. CG)	D250-LH2
$x_{root,LE}$ [m]	16.54	21.62	22.84	16.05	20.11	19.60
S_h [m^2]	24.72	36.74	47.20	25.05	32.64	37.02
ξ_{mg} [-]	0.80	0.80	0.80	0.96	1.05	1.23
MFM [kg]	9123	3835	3930	9207 (+0.9%)	3816 (-0.5%)	3820 (-2.8%)

[34]. This leads to a total of two configurations for the D250 and four configurations for the D250-LH2. The table summarizes the resulting geometric variations, with particular emphasis on wing position and horizontal tailplane area, as these represent the main values affected by changes in landing gear integration and CG range. The table also depicts the value for the relative position of the main landing gear with respect to the wing, ξ_{mg}. These geometric changes are directly linked to aircraft performance, which is evaluated in terms of block fuel for the mission, using mission fuel mass (MFM) as the primary performance metric. The results are presented for the point design and provide an initial indication of the relative performance of the different configurations. The corresponding trends for the shorter family members are not shown, as they follow the same behavior.

For the D250 baseline, both landing gear integration concepts show comparable performance, with the wing-mounted configuration achieving less than a 1% improvement in mission fuel mass. These results exclude trim drag, which would likely penalise the wing-mounted concept due to its increased static margin (17.5% MAC versus 10% MAC). Within modelling uncertainties, no clear selection can be made based on performance alone. However, the wing-mounted configuration may still be preferred due to improved fuselage aerodynamics, better turning stability, and more efficient cargo space utilisation, consistent with typical industry practice for low-wing aircraft.

For the reduced-CG D250-LH2 case, both configurations again show similar performance, although the wing-mounted design exhibits slightly lower performance in this case. The optimal landing gear position shifts aft to $\xi_{mg} = 1.05$ (compared to 0.96 for the kerosene baseline). Consequently, the forward shift of the wing is more limited for the LH2 design, as the gear remains constrained at the $\xi_{mg} = 0.8$ limit. This results in a more pronounced difference between the horizontal tailplane areas of the two landing gear integration solutions.

When the CG range constraint is removed, performance degrades for both configurations, but more strongly for the wing-mounted case. The optimal landing gear position moves further aft to $\xi_{mg} = 1.23$, while the wing-mounted design remains constrained at $\xi_{mg} = 0.8$. Consequently, the wing position is severely limited. For the D250 baseline, the difference in wing position between the two landing gear integration solutions was approximately 0.5 m. For the D250-LH2, this difference increases to almost 3 m, meaning the wing is positioned almost 3 m aft of its optimum location. Therefore, a wing-mounted landing gear configuration without operational constraints leads to an unfeasible solution for the D250-LH2. The unfavourable wing position results in an impractically large horizontal tailplane, yielding a 3% lower efficiency for the same mission compared to the fuselage-mounted design (note that these results do not account for trim drag, which further strengthens this conclusion). In the fuselage-mounted configuration, the horizontal tailplane also increases under unconstrained CG conditions; however, since the main gear position is not fixed, the overall performance impact is smaller.

Overall, the results indicate that a wing-mounted landing gear configuration is preferred for conventional designs (like the D250), as the favourable aircraft characteristics outweigh the sub-optimal HTP size and wing position. Fuselage-mounted gear solutions, on the other hand, should be considered when they offer clear performance advantages, which is the case for the D250-LH2 aircraft concept. Improved performance, together with the possibility of increasing the CG range without major penalties, are the deciding factors.

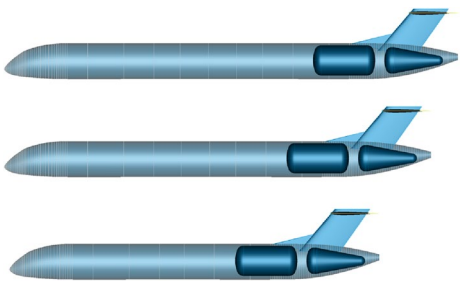


Fig. 15 D250-LH2 family concept with constant fuel capacity and varying payload

5.2 D250 and D250-LH2 family results

Two shorter family variants are derived from both concepts following the requirements in Table 7. The family design strategy follows the same approach as for the D239, where payload is varied through fuselage length while maintaining a constant fuel tank capacity, resulting in a payload–range trade-off for the shorter variants. The D250 and D250-LH2 (Figures 10 and 11) serve as the reference member.

The family strategy selected for the D250-LH2 concept follows the conventional approach used in industry for kerosene-powered aircraft. An example of the resulting LH2 family design is shown in Figure 15. Unlike the D250 family, the ranges of the D250-LH2 mid and short variants are not prescribed, but instead a result from the fixed tank capacity, which is sized for the 1500 NM design mission of the long family member, and the associated reduction in payload. The resulting foam-insulated aluminium tanks achieve gravimetric efficiencies of up to 54 % (Table 9). The gravimetric efficiency values given do not consider masses originating from tank mounting and tank systems. The remaining family definitions are identical to the D250 baseline (Table 7). Due to the limited payload–range flexibility imposed by the cryogenic tank configuration, additional

Table 9 D250-LH2 family tank characteristics

Value	Forward	Aft	Unit
Shell material	Aluminium		-
Insulation material	Foam		-
Shape	Cylinder	Cone	-
Max. pressure	2.0		bar
Sizing volume	47.8	17.8	m^3
Outer radius	1.68	1.46	m
Empty mass	2457	1210	kg
Max. fuel mass	2935	1100	kg
Unusable fuel	170	63	kg
Gravimetric efficiency	54	48	%

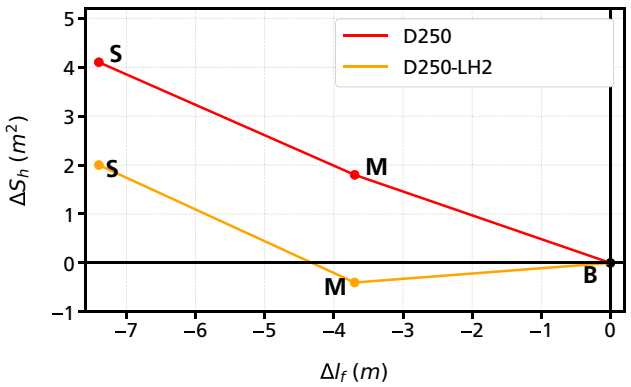


Fig. 16 Point design results for the required HTP area as a function of the change in fuselage length for both D250 and D250-LH2 family concepts. Results are shown for all base (or long) (B) mid (M) and short (S) family variants

family strategies with a lower degree of commonality, i.e. without shared tank, are explored in section 5.3.

Figure 16 depicts the relationship between change in HTP area and reduction in fuselage length. It is shown for both the D250 and D250-LH2 concepts and their respective shorter variants. The base (long) family member serves as a reference for the variations in fuselage length and HTP area.

The findings from the D239 analysis in Section 4 are confirmed for the D250 baseline family. A established trend in HTP sizing for kerosene aircraft families is observed: a reduction in fuselage length leads to a shorter tail moment arm and, consequently, a larger required HTP. As a result, the short family member typically governs the HTP sizing.

Despite the D250-LH2-short is still sizing for the HTP, the aforementioned ascending trend is not exactly mimicked for the D250-LH2 family. The reason behind relies on the noticeable variation of the CG range with fuselage length that is given for an LH2 aircraft family. For an LH2 concept, the tank position relative to the wing increases with fuselage length. When the fuselage is stretched, the tank is shifted backwards a distance equal to Δl_f, whereas the wing is only shifted backwards a distance equal $\Delta l_f - \Delta l_{VTP}$. Therefore, a larger longitudinal CG range results for the stretched

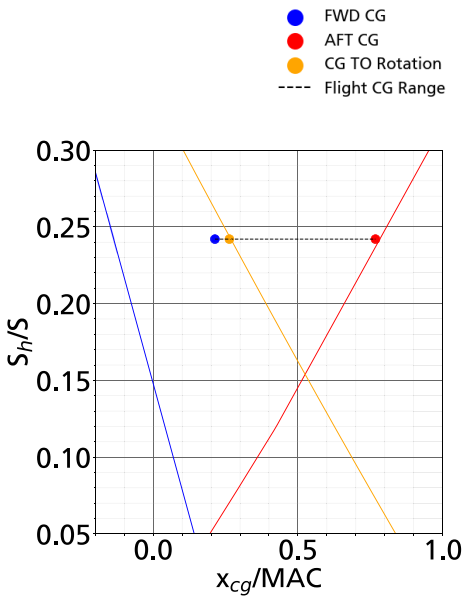


Fig. 17 Scissors plot for the D250-LH2 concept (Point design)

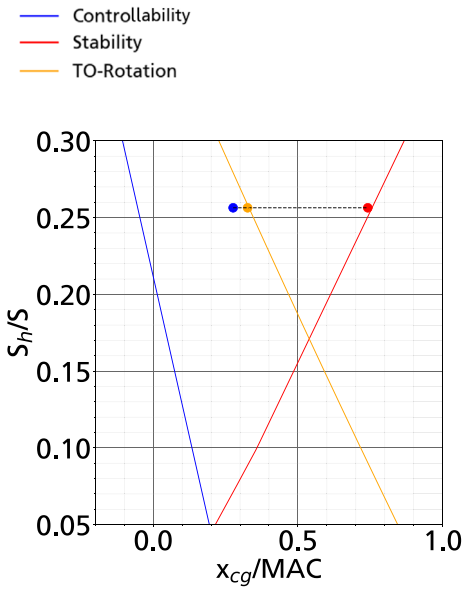


Fig. 18 Scissors plot for the D250-LH2-short (Point design)

family member. Figures 17 and 18 present the scissors plots for the long and short members of the D250-LH2 family.

Two effects are given for the shortest member, when compared to the long. On the one hand, the shorter fuselage results in a smaller lever arm. The shorter lever arm decreases the amplitude between the bounds of the scissors plot, limiting the allowable CG range for a given HTP area. This effect mirrors the behaviour observed in the kerosene family. On the other hand, the CG range is also shorter for the short family member. For the D250-LH2, the CG range is around 60% of the MAC, and reduces to around 50% for the -short. This effect is only given for LH2 aircraft due

to its tank position. For a kerosene family, the fuel mass is positioned in the wing, resulting in similar longitudinal CG ranges among all members (see scissor plots for the D239 family in Figs. 8, 9). In the end, the lever arm effect is compensated by the shortened CG range, resulting into a smaller HTP area variation compared to the D250 baseline. As observed in Fig. 16, the increment in HTP area due to the same fuselage length reduction for the D250-LH2, is halved compared to the D250. The same trend is observed for the D250-LH2-mid, which also has a shorter lever arm together with a shorter CG range. For this concept, the resulting HTP area does not change, despite the reduction of 3.7 meters in fuselage length.

Since the short variant remains the sizing case for the empennage, the HTP and VTP areas (for both the D250 and D250-LH2 families) are used to resize all family members following the methodology described in Chapter 2 until convergence is achieved. While the shortest configuration continues to govern both horizontal and vertical tailplane sizing, a different behaviour is observed for LH2 compared to kerosene aircraft. This motivates the quantification of empennage commonality effects by evaluating the block fuel penalty of the family design relative to the corresponding point-optimized configurations, as done in Sect. 4 for the D239 reference family. Table 10 compares the final D250 and D250-LH2 family designs to the point designs. As observed for the D239 reference family, the long (main) family member is the one with the biggest performance penalty due to empennage commonality (see Table 5), thus only the long family member is shown in this case for simplification.

Both family designs exhibit a similar increase in operating empty mass (OEM) of approximately 0.7–0.8% to maintain empennage commonality across variants. Although the variation in empennage size is smaller for the D250-LH2 family compared to the D250 baseline (Fig. 16), the resulting OEM increment remains comparable in both relative and absolute terms. To better understand the origin of this increase in the LH2 case, Fig. 19 presents a breakdown of the OEM increment by component, expressed as a percentage of the total increase, for both the D250 and D250-LH2 main family members.

The change in OEM due to the empennage for the LH2 design is indeed smaller. However, there are mass changes that are given for an LH2 aircraft family design that are not given in the case of the kerosene family. As explained before, the D250-LH2 tank is sized for the design mission. Thus, fitting a larger empennage results into an enlarged tank and longer fuselage to still fulfil the range for the design mission. This corresponds to almost 25 % of the total increase. However, the impact that the OEM increment has on the performance is lower for the LH2 design. Fuel consumption is more sensitive to an oversized HTP than to a heavier fuselage and tanks. As a result, the fuel penalty for the same family design strategy is halved for the LH2 design. For the same fuselage length reduction, the penalty on the long member is 1% for the D250-LH2 when comparing the final family design to the corresponding optimized point design, while being 2.04 % for the D250 baseline. Tailplane commonality is feasible for an LH2 aircraft family with shared tanks, and results in a smaller penalty than for conventional designs.

The performance penalty associated with tailplane commonality for the D250 baseline results in a 2% increase in mission fuel mass (MFM). This value represents a marginal increment over the penalty observed for the D239 reference (1.6%). Such a trend suggests that for next-generation aircraft featuring high-aspect-ratio wings, the reduction in inner wing chord length and the subsequent trade-offs required for landing gear integration, may amplify the performance decrement when the empennage is shared across family members. Conversely, the proximity of these results suggests that the benefits of commonality remain consistent between the two families.

Table 10 Comparison of D250 and D250-LH2 point and family designs (long variant)

	Point design		Family design	
	D250	D250-LH2	D250	D250-LH2
$x_{root,LE}$ [m]	16.54	19.50	16.51	19.94
S_v [m^2]	17.38	20.39	21.12	21.41
S_h [m^2]	24.72	37.02	29.90	39.00
Payload [kg]	23750	23750	23750	23750
OEM [kg]	47199	56497	47561 (+ 0.77%)	56890 (+ 0.73%)
MTOM [kg]	80073	84038	80621 (+ 0.68%)	84464 (+ 0.54%)
MFM [kg]	9123	3820	9310 (+ 2.04%)	3856 (+ 1.0%)

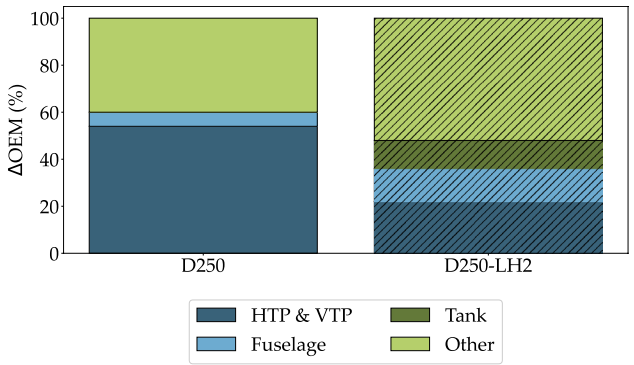


Fig. 19 OEM-breakdown by component increment due to tailplane commonality for the D250 and D250-LH2

To conclude, a comparison between the final D250 and D250-LH2 aircraft concepts is shown in Fig. 20. This figure illustrates key architectural differences, specifically in HTP area, fuselage length, and landing gear integration. For a more detailed comparison, Appendix A provides comprehensive three-view drawings of both designs. The HTP area for a hydrogen aircraft with rear tanks is substantially larger than for a kerosene aircraft. Based on the plots on Figs. 17 and 18, the take-off rotation requirement is the main driver for the HTP sizing process. It is significantly more restrictive than the controllability requirement, being clearly the limitation for the most forward CG of the aircraft. The aft landing gear position characteristic of LH2 concepts with rear tanks results in a short tail lever arm, which significantly increases the HTP area that is required for rotation. Even for this case, in which the HTP for the kerosene baseline was not minimized due to landing gear integration issues, the volume coefficient is more than 40% larger. The values of the HTP area and volume coefficient for all main family members designed in this study are compared in Table 11. Note that the values presented in the table are those for the point design, without considering potential family members. This allows for a better comparison between the LH2 and kerosene designs, focusing purely on the different aircraft mass distribution and its impact on tailplane area from a flight mechanics perspective.

5.3 Hydrogen aircraft family design space exploration

The D250-LH2 family designed in Sect. 5.2 from the D250-LH2 concept, is further studied in this section. The goal is to identify trends in empennage commonality among family members by comparing different family strategies. In the previous sections, the conventional family approach of constant fuel capacity with varying payload has been analysed. In this case, for kerosene aircraft, the fuel requirements are usually defined for the stretched version. Since kerosene is stored in wing volumes that typically exceed design mission requirements, conventional aircraft feature a surplus of fuel capacity. This allows smaller variants with lower structural and payload weights to leverage this extra volume for extended range or operational flexibility [5]. In contrast, the LH2 family is volume-constrained. To avoid the substantial drag and structural weight penalties associated with oversized tanks [6], the maximum fuel capacity is precisely matched to the design mission fuel mass of the largest family member. Consequently, the range is no longer a TLAR for the shrinked family variants but a fixed result of the shared tank capacity. The payload-range diagrams in Fig. 21 illustrate the difference between kerosene and LH2 family designs. The base (long) family members are

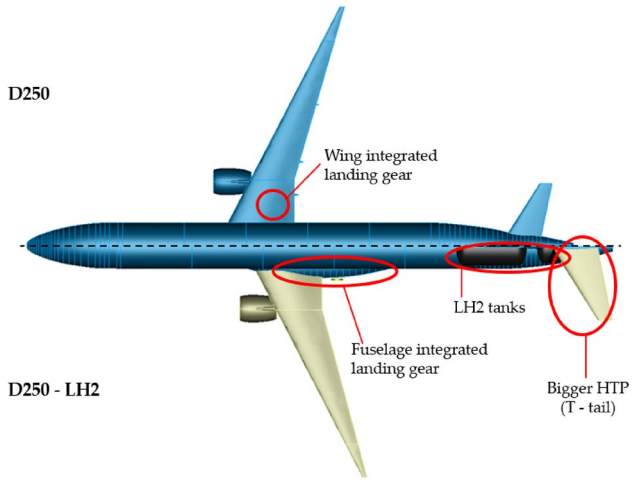


Fig. 20 D250-LH2 (bottom) and D250 (top) concepts

Table 11 Comparison of key horizontal tail parameters for D239, D250, and D250-LH2 aircraft concepts

	D239	D250	D250-LH2	Units
S_h	26.20	24.72	37.02 (+ 47.8%)	m^2
c_{HT}	1.0	1.2	1.7 (+ 42.5%)	–

compared to the shorter variants of all families from Sects. 4, and 5.2.

A notable difference arises in the length of the substitution segment, where payload mass is inverted to fuel mass to gain range. For kerosene-powered variants, the short members exhibit a longer substitution segment. In contrast, for the LH2 aircraft, the substitution segments of both the long and short variants are approximately equal in length. Consequently, kerosene aircraft families following the classic design strategy of keeping a constant fuel capacity can cover a much wider range spectrum than their LH2 counterparts. From an airline's perspective, the latter may therefore appear less attractive, as they exhibit lower payload–range flexibility and are unable to cover as many routes as their kerosene equivalents. Therefore, it is reasonable to consider LH2 family design strategies that account for different tank sizes.

In this section, two more design strategies are explored and compared regarding tailplane commonality to the one shown in Fig. 15. The first one considers constant payload and increased fuel capacity. An extended range version (ER) is derived from the main family member. The second strategy considers a variation of both payload and range among family derivatives. In this case, the payload is reduced compared to the main family member, while the tank capacity is increased. It focuses on a scenario where the market demands a family of aircraft with range requirements for the shorter version that exceed what can be achieved with shared tanks. Kerosene aircraft do not usually follow this design approach, as shorter variants generally have relaxed

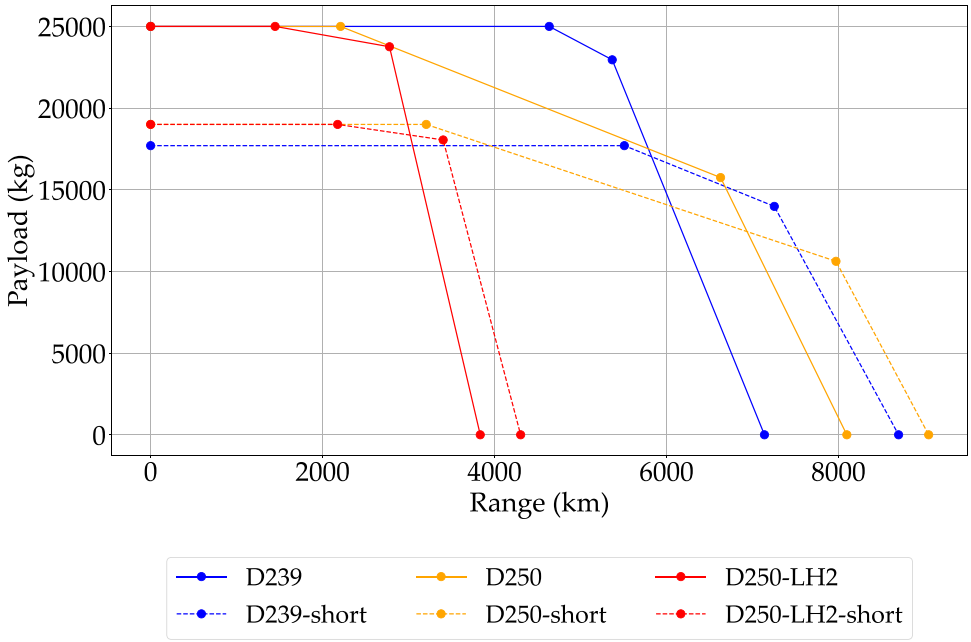


Fig. 21 Payload-range diagram comparison for the -long and -short members from the D239, D250, and D250-LH2 families

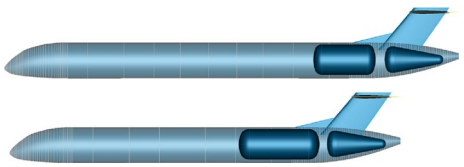


Fig. 22 LH2 family concept with constant payload and varying fuel capacity. D250-LH2 (top) and D250-LH2-ER (bottom)

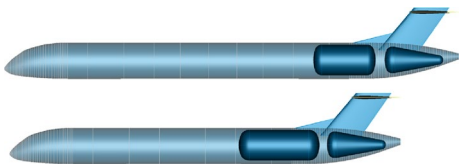


Fig. 23 LH2 family concept with varying fuel capacity and payload. D250-LH2 (top) and D250-LH2-ER-short (bottom)

range limitations. A common practice for such aircraft is increasing both the fuel capacity and payload of the base member. Replicating this for the D250-LH2 concept is not feasible, as the aircraft fuselage would quickly reach fineness ratio exceeding the state of the art. A switch to a twin aisle fuselage concept is required at some point, which is out of the scope for this publication. Therefore, the strategy of reducing payload and increasing range is studied. Based on the results, some final conclusions can be drawn for the strategy in which both are increased. A representation of both families is shown in Figs. 22 and 23. The main member (D250-LH2) is sketched on top.

Other authors, such as Huete et al. [15] or Almarzooqi et al. [16], have adopted a constant-fuselage-length approach to LH2 aircraft family design, in which payload–range flexibility is achieved by varying the proportions of pressurized and unpressurized fuselage sections. However, this fixed-fuselage approach imposes significant design constraints. With a constant fuselage length, payload and range become strongly coupled through the fixed internal volume, limiting the ability to independently specify both as design requirements. Additionally, varying tank size within a fixed fuselage does not provide meaningful commonality benefits. Although the external geometry remains unchanged, differences in tank dimensions and the associated repositioning of pressure bulkheads result in substantial internal redesign across family members. These limitations, both in terms of requirement flexibility and effective commonality, together with the fact that this approach does not reflect established kerosene aircraft family design practices, motivate its exclusion from the present study. Instead, the focus is placed on more conventional family strategies based on shared tank configurations (see previous sections), as well as on approaches that increase tank size (Figs. 22 and 23). These strategies provide greater insight into mitigating the payload–range flexibility limitations inherent to LH2 aircraft, while remaining consistent with industry practices such as extended-range (ER) variants in kerosene-powered aircraft.

Increasing tank size leads to a wider CG range. Consequently, both the D250-LH2-ER and D250-LH2-ER-short configurations drive the sizing of the HTP for the overall aircraft family. In previous analyses, the D250-LH2-short variant was also found to size the tailplane, resulting in a block fuel penalty of approximately 1% due to tailplane commonality for the main family variant (about half the penalty observed for the kerosene design). The next step is to evaluate how reducing the degree of commonality by allowing variations in tank size affects this performance

penalty. For kerosene-powered aircraft, the strategies discussed earlier neither reduce the tail moment arm nor significantly increase the CG range. Fuel capacity can typically be increased by adding a center tank, which has only a limited effect on mass distribution and CG position. As a result, such configurations do not pose significant challenges for tailplane commonality.

Figure 24 illustrates the impact of increasing fuel capacity on both HTP area and the associated block fuel penalty due to empennage commonality, comparing the final D250-LH2 family design with the optimized configuration. Results are shown for both the D250-LH2-ER (Fig. 22) and D250-LH2-ER-short (Fig. 23) variants.

The two configurations differ only in payload: the former retains the baseline payload, while the latter reduces it by 60 passengers. A sensitivity analysis was performed by varying the fuel capacity from the baseline value of 3800 kg of LH2 and tracking the resulting changes in tailplane area. The variation in fuel is expressed as the change in tank mass and associated systems ($\Delta m_{\mathrm{LH2,sys}}$). All results are referenced to the D250-LH2 optimized point design, which has a tank mass of 5900 kg and an HTP area of 37.1 m^2.

The HTP area of the -ER variants is significantly more sensitive to changes in tank mass than that of the -ER-short configurations. Counterintuitively, integrating a larger tank while reducing payload (and fuselage length) has a smaller impact on HTP commonality than maintaining the original payload. This is because reducing fuselage length limits the increase in CG range, despite the shorter tail lever arm. HTP sizing is highly sensitive to CG range, and increases in CG excursion can offset the benefits of a longer lever arm. This trend is consistent with earlier findings in Sect. 5.2. Based on the results from Fig. 24, it can be concluded that the most critical case for LH2 aircraft family tailplane commonality arises when both payload and range are increased. In such configurations, a longer fuselage combined with a larger tank significantly expands the CG range, driving higher HTP sizing requirements and shifting the landing gear further aft. This behavior contrasts with kerosene-powered aircraft, where increasing fuselage length primarily improves the lever arm and reduces tail size requirements.

In summary, increasing tank size alone can be tackled, particularly if fuselage length is reduced to limit CG variation. However, increasing both tank size and fuselage length, or maintaining fuselage length while enlarging the tank, leads to larger CG ranges that negate lever arm benefits and result in significant HTP commonality penalties.

6 Conclusions and outlook

This paper adapted the industry approach of tailplane commonality into the DLR methodology for preliminary aircraft design. The enhanced aircraft design workflow can simultaneously size three aircraft while enforcing common horizontal and vertical tailplanes. This improved methodology enables a better understanding of the interaction between tailplane sizing and commonality in the design of LH2 aircraft families equipped with rear-fuselage tanks, allowing the associated performance penalties in terms of block fuel to be compared with those of conventional kerosene aircraft.

In kerosene-powered aircraft families following the conventional design strategy of constant fuel capacity, the short-fuselage variant typically defines the required horizontal and vertical tailplane areas. This occurs because of the reduced tail moment arm, which necessitates larger surfaces to satisfy stability and control requirements. This trend was corroborated during the sizing of the D239 and D250 families. In both cases, a moderate mission fuel mass penalty of approximately 2% was observed for the long-family

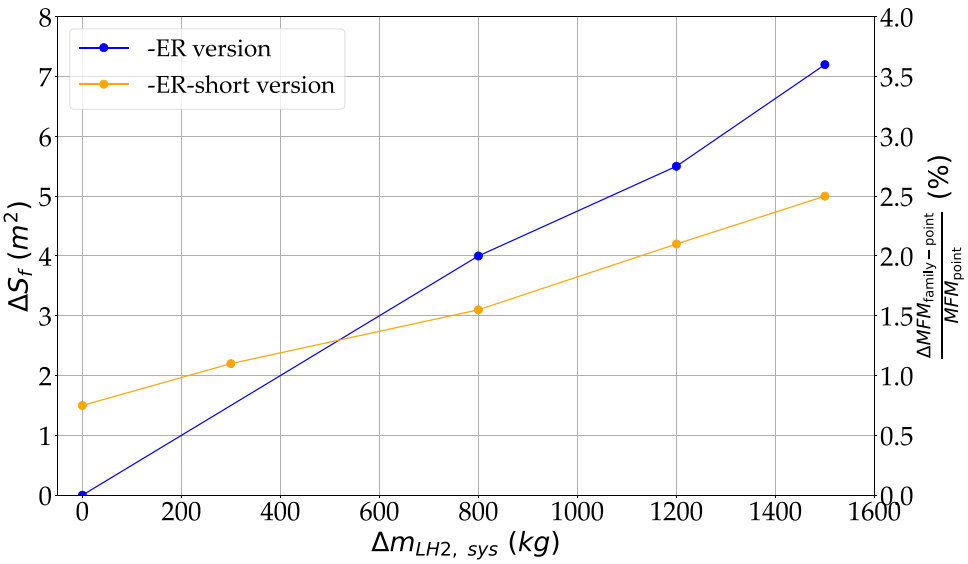


Fig. 24 Effect of tank mass increase on HTP area and empennage commonality block fuel penalty for D250-LH2-ER and ER-short variants

derivatives when utilizing a common empennage, with respect to the optimized point designs. This is considered a reasonable trade-off, as it aligns with the commonality strategies of existing commercial aircraft families.

However, for LH2 aircraft families using the same strategy, the positioning of the tanks and their impact on the aircraft's overall CG range, alters the trends observed in kerosene designs. The tail moment arm effect changes, and a shorter arm no longer necessarily results in a larger horizontal tailplane. A shorter fuselage brings the wing and tank closer together, reducing the CG range, which partially compensates the reduction in tail lever arm. In the case of the D250-LH2 aircraft family, derived using the same strategy as the kerosene D250 family, the short-fuselage variant remains the sizing case for both the horizontal and vertical tailplanes. However, the resulting block fuel penalty associated with tailplane commonality is reduced by approximately 50% compared to the D250 kerosene reference case, when comparing the final LH2 family design to the corresponding optimized point design of the D250-LH2 configuration. The difference in optimal HTP area among members is smaller, due to the counteracting effects of reduced lever arm and reduced CG range of the -short.

The achievable gravimetric and volumetric energy densities of the LH2 storage system, and the fact that it is typically sized for the design mission of the largest family variant, results in limited payload–range flexibility of the family when compared to kerosene aircraft families with constant fuel capacity. Therefore, it is reasonable to consider family design strategies with different tank sizes among the various members. In contrast to the observations made for the constant fuel capacity family strategy, design strategies that involve increasing fuel capacity, payload, or both, now require special attention when sizing an LH2 family with a common tailplane. Conversely to kerosene families, all cases result in increased CG ranges due to the tank positioning. The HTP area appears to be highly sensitive to variations in the CG range, even more so than to changes in the tail lever arm. Consequently, significant challenges are anticipated in achieving tailplane commonality.

A critical observation regarding the designs considered in this study and the resulting conclusions is the assumption of full CG range coverage. Under this assumption, a fuselage-mounted landing gear was found to provide the best compromise for an LH2 aircraft with rear tanks, as it allows an optimal wing position, a feasible HTP area, and no operational limitations. However, reducing the CG range through the strategic use of trim weight represents a viable alternative to avoid the extremely aft CG positions as explained in section 5.1. Adopting such an approach may have different implications for empennage commonality within the aircraft family. Furthermore, the influence of trim drag remains a decisive factor in performance validation. Incorporating trim drag into the modelling process would significantly refine the evaluation of the various design concepts, particularly for wing-mounted gear configurations which often exhibit high static margin values.

At a broader level, this work highlights the significant potential of empennage commonality in LH2 aircraft families, providing initial guidelines for the design of such families. Future research should therefore focus on expanded design space exploration, including the interaction between CG management, landing gear integration strategies, and their impact on empennage sizing. In addition, operational strategies and regulatory considerations should be further investigated. Such developments would strengthen the applicability of the present methodology and support the design of LH2 aircraft families with a high degree of commonality.

One final remark can be made on the methodology side. The additional outer convergence loop for the family significantly increases the calculation effort. Since the tailplane is sized for the whole family, all aircraft design loops are triggered multiple times to converge to a common tailplane size, resulting in a calculation time that is roughly doubled to tripled when compared to a family design in which empennage commonality is not considered. Future work can focus on estimating the empennage size for the family already within the main aircraft design loop, avoiding the need to recalculate the complete family version designs afterward. This would lead to a calculation time comparable to a process in which commonality is not considered.

Appendix

Appendix A: Three-dimensional views: D239, D250 and D250-LH2 final family conceptual designs

The appendix details the primary aircraft concepts via standard plan, front, and side views, with its corresponding general dimensions.

- D239 Family (Figs. 25 and 26): Display the reference D239 and its shortened variant. Both share a tail sized for the D239-short.
- D250 Family (Fig. 27): Shows the final design of the D250 main family member, with wing-integrated landing gear and an empennage sized for the short variant.
- D250-LH2 Family (Fig. 28): Depicts the final design of the D250-LH2 main family member. The gear is

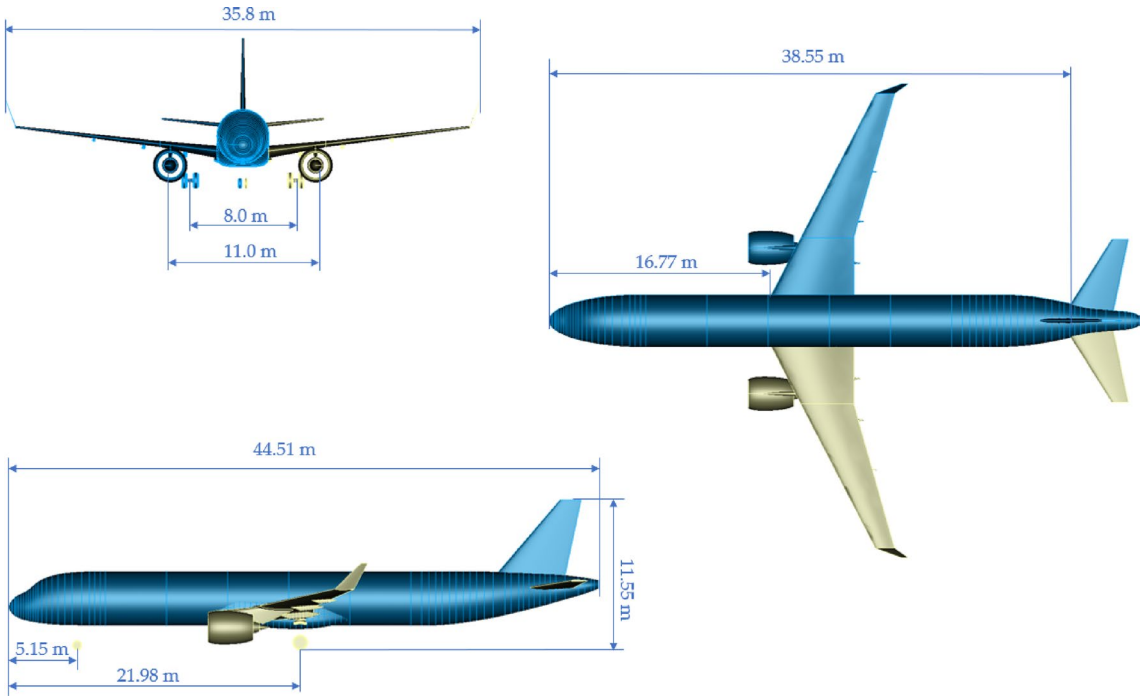


Fig. 25 Three standard views for the D239 final concept

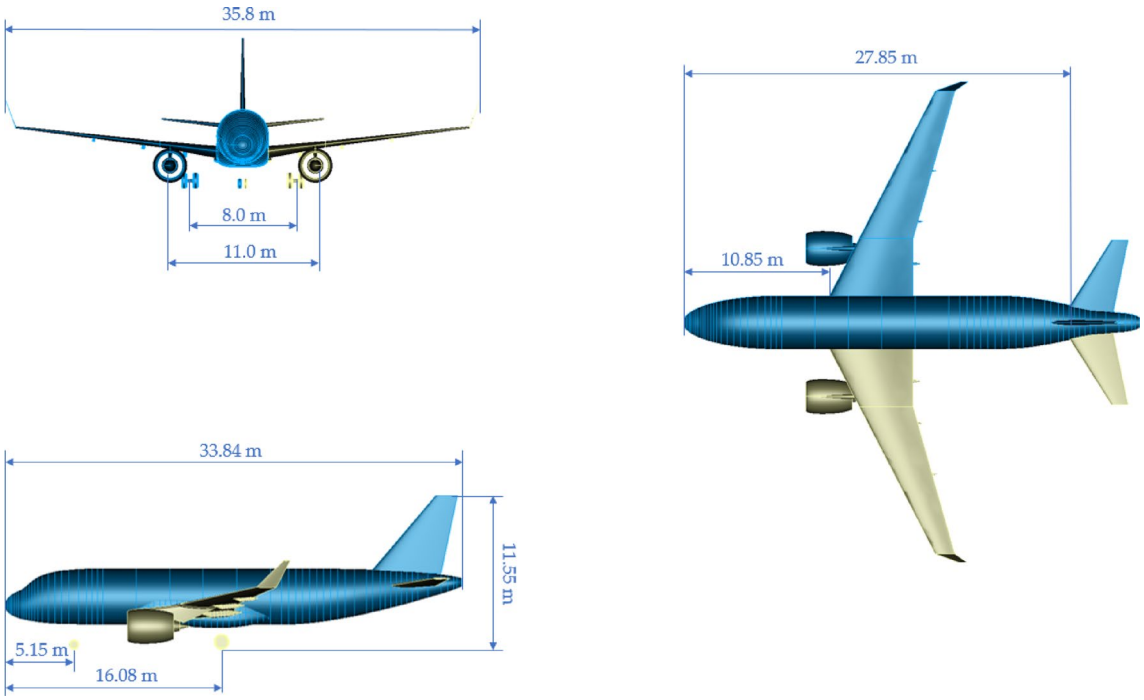


Fig. 26 Three standard views for the D239-short final concept

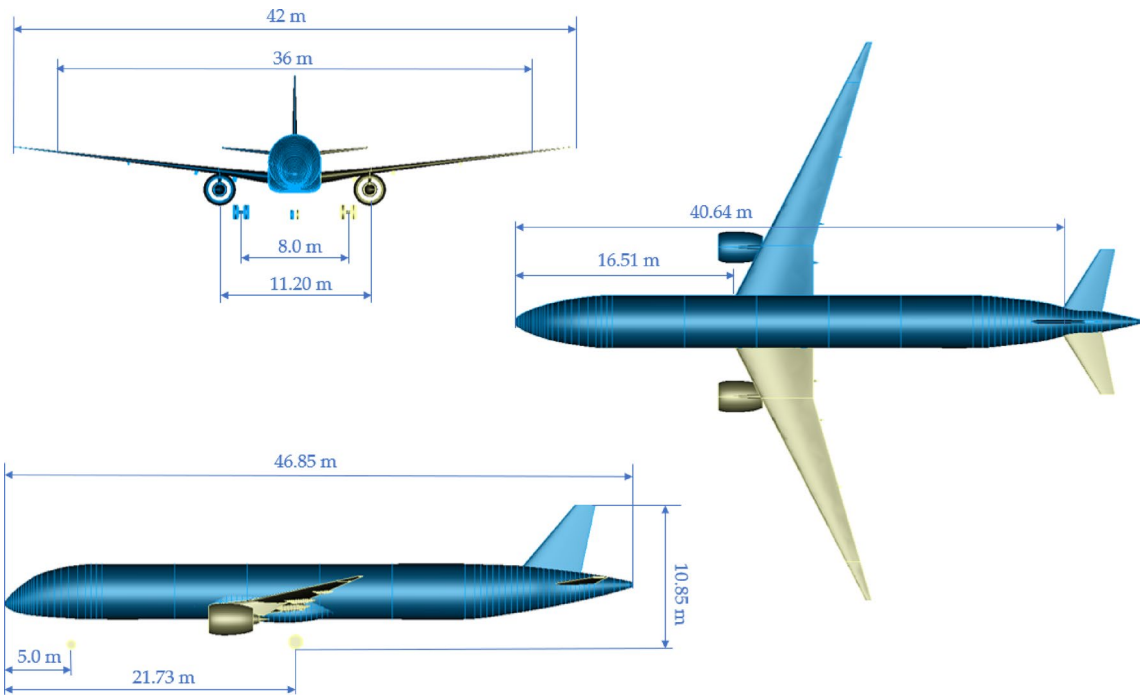


Fig. 27 Three standard views for the D250 final concept

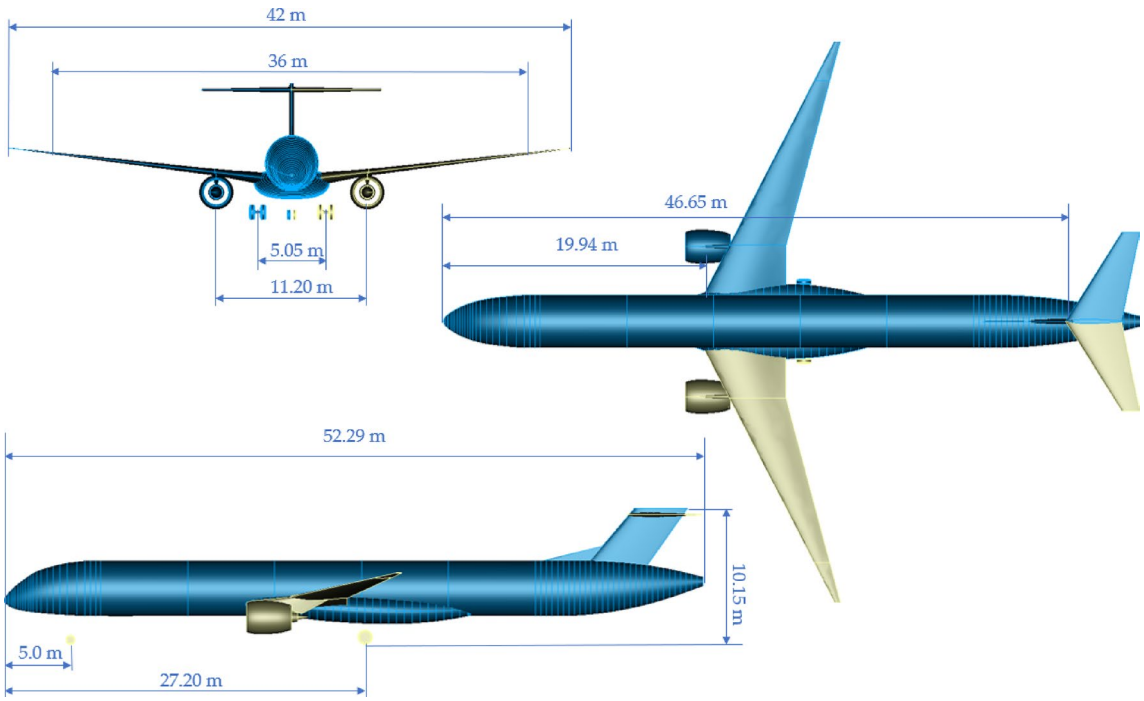


Fig. 28 Three standard views for the D250-LH2 final concept

integrated in this case into the fuselage. The tailplane is still sized for the shorter variant (D250-LH2-short).

Author contributions A.G.M., F.F., and D.S. conceived the study and defined the research methodology. A.G.M. performed the design studies, and elaborated the figures. F.F., D.S., and S.A. revised the designs, and implemented their feedback. The first draft of the manuscript was written by A.G.M.. S.A., F.F., and D.S. contributed to manuscript revision and technical discussion. All authors reviewed and approved the final manuscript.

Funding Open Access funding enabled and organized by Projekt DEAL.

Data availability No datasets were generated or analysed during the current study.

Declarations

Conflict of interest The authors have no conflict of interest to declare that are relevant to the content of this article.

Open Access This article is licensed under a Creative Commons Attribution 4.0 International License, which permits use, sharing, adaptation, distribution and reproduction in any medium or format, as long as you give appropriate credit to the original author(s) and the source, provide a link to the Creative Commons licence, and indicate if changes were made. The images or other third party material in this article are included in the article's Creative Commons licence, unless indicated otherwise in a credit line to the material. If material is not included in the article's Creative Commons licence and your intended use is not permitted by statutory regulation or exceeds the permitted use, you will need to obtain permission directly from the copyright holder. To view a copy of this licence, visit http://creativecommons.org/licenses/by/4.0/.

References

1. Tiwari, S., Pekris, M.J., Doherty, J.J.: A review of liquid hydrogen aircraft and propulsion technologies. Int. J. Hydrogen Energy **57**, 1174–1196 (2024). https://doi.org/10.1016/j.ijhydene.2023.12.263
2. Adler, E.J., Martins, J.R.: Hydrogen-powered aircraft: Fundamental concepts, key technologies, and environmental impacts. Prog. Aerosp. Sci. **141**, 100922 (2023). https://doi.org/10.1016/j.paerosci.2023.100922
3. Verstraete, D., Hendrick, P., Pilidis, P., Ramsden, K.: Hydrogen fuel tanks for subsonic transport aircraft. Int. J. Hydrogen Energy **35**(20), 11085–11098 (2010). https://doi.org/10.1016/j.ijhydene.2010.06.060
4. Wöhler, S., Burschyk, T., Häßy, J., Iwanizki, M.: Design and assessment of long range aircraft concepts with focus on fossil kerosene, sustainable aviation fuel and liquid hydrogen as energy carriers. In: AIAA Aviation Forum (San Diego, California, USA, 2023). https://doi.org/10.2514/6.2023-3229
5. Westenberger, A.: LH2 as Alternative Fuel for Aeronautics – Study on Aircraft Concepts. Final report cryoplane project, Airbus Deutschland GmbH (2008). https://www.semanticscholar.org/paper/LH2-as-Alternative-Fuel-for-Aeronautics-Study-on-Westenberger-Deutschland/bbda93f6df116ae82d32ada43dacb41786e7ba59
6. Onorato, G., Proesmans, P., Hoogreef, M.F.M.: Assessment of hydrogen transport aircraft: Effects of fuel tank integration. CEAS Aeronaut. J. **13**(4), 813–845 (2022). https://doi.org/10.1007/s13272-022-00601-6
7. Yongjie, Z., Yongqi, Z., Kang, C., Wenjun, D., Dayong, D.: A review of the development of civil aircraft family. J. Phys: Conf. Ser. 1877, (2021). https://doi.org/10.1088/1742-6596/1877/1/012024
8. Riaz, A., Guenov, M.D., Molina-Cristobal, A.: Set-based approach to passenger aircraft family design. J. Aircr. **54**(1), 310–326 (2017). https://doi.org/10.2514/1.C033747
9. The Boeing Company: 777 Passenger: The Boeing 777 History. https://www.boeing.com/content/dam/boeing/boeingdotcom/company/about_bca/startup/pdf/historical/777_passenger.pdf (2009)
10. Torenbeek, E.: Synthesis of Subsonic Airplane Design, 1^{st} ed. edn, Kluwer Academic Publishers (1982)
11. Airbus: Airport Planning Manual: Airbus A319. (2021). Online. https://aircraft.airbus.com/sites/g/files/jlcbta126/files/2025-01/AC_A319_0624.pdf Accessed 2024-04-04
12. Airbus: Airport Planning Manual: Airbus A320. (2021). Online. https://aircraft.airbus.com/sites/g/files/jlcbta126/files/2025-01/AC_A320_0624.pdf Accessed 04 Apr (2024)
13. Airbus: Airport Planning Manual: Airbus A321. (2021). Online. https://aircraft.airbus.com/sites/g/files/jlcbta126/files/2023-12/ac_a321_1223.pdf Accessed 04 Apr (2024)
14. Airbus: Airport Planning Manual: Airbus A350. (2021). Online. https://aircraft.airbus.com/sites/g/files/jlcbta126/files/2023-02/Airbus-Commercial-Aircraft-AC-A350-900-1000.pdf Accessed 15 Jan (2024)
15. Huete, J., Nalianda, D., Pilidis, P.: Propulsion system integration for a first-generation hydrogen civil airliner? Aeronaut. J. **125**(1291), 1654–1665 (2021). https://doi.org/10.1017/aer.2021.36
16. Almarzooqi, R., VonFeldt, M.J., Kallou, E., Xie, J., Gladin, J.C., Mavris, D.: Design and evaluation of an aircraft family with diverse energy sources for sustainable aviation. In: AIAA SCITECH Forum, Orlando, Florida, USA (2025). https://doi.org/10.2514/6.2025-1247
17. DLR: DLR EXACT: Project Overview (2024). https://exact-dlr.de/project-overview/ Accessed 14 Sep (2024)
18. Atanasov, G., Wehrspohn, J., Kühlen, M., Cabac, Y., Silberhorn, D., Kotzem, M., Dahlmann, K., Linke, F.: Short-medium-range turboprop-powered aircraft as a cost-efficient enabler for low climate impact. In: AIAA Aviation Forum (San Diego, CA, USA, 2023). https://doi.org/10.2514/6.2023-3368
19. Ramm, J., Pohya, A.A., Wicke, K., Wende, G.: Uncertainty quantification in hydrogen tank exchange: Estimating maintenance costs for new aircraft concepts. Int. J. Hydrogen Energy **68**, 159–169 (2024). https://doi.org/10.1016/j.ijhydene.2024.04.157
20. Fröhler, B., Häßy, J., Abu-Zurayk, M.: Development of a medium/long-haul reference aircraft. CEAS Aeronaut. J. **13**, 693–713 (2023). https://doi.org/10.1007/s13272-023-00662-1
21. Wöhler, S., Atanasov, G., Silberhorn, D., Fröhler, B., Zill, T.: Preliminary aircraft design within a multidisciplinary and multifidelity design environment. In: Aerospace Europe Conference (Bordeaux, France, 2020). https://elib.dlr.de/140902/
22. Fröhler, B., Wöhler, S., Zill, T., Iwanizk, M.: Increasing fuel efficiency for short to medium range market: A conceptual aircraft design study on unconventional configurations. In: AIAA Aviation Forum (2024). https://doi.org/10.2514/6.2024-4325
23. Fröhler, B., Hesse, C., Atanasov, G., Wassink, P.: Disciplinary sub-processes to assess low-speed performance and noise characteristics within an aircraft design environment, German Aerospace Congress (DLRK (2020). https://doi.org/10.25967/530201
24. Burschyk, T., Silberhorn, D., Wehrspohn, J., Kühlen, M., Zill, T.: Scenario-based implications of liquid hydrogen storage tank

insulation quality for a short-range aircraft concept. In: AIAA Aviation Forum (San Diego, California, USA, 2023). https://doi.org/10.2514/6.2023-3522
25. Hecken, T., Balack, P., Petsch, M., Zerbst, D.: Conceptual loads assessment of aircraft with fuselage integrated liquid hydrogen tank. In: German Aerospace Congress (DLRK) (Dresden, Germany, 2022). https://elib.dlr.de/189171/
26. Balack, P., Hecken, T., Petsch, M., Atanasov, G., Silberhorn, D., Nagel, B.: Semi-physical method for the mass estimation of fuselages carrying liquid hydrogen fuel tanks in conceptual aircraft design. In: German Aerospace Congress (DLRK) (Dresden, Germany, 2022). https://elib.dlr.de/203339/
27. Zerbst, D., Hecken, T., Balack, P., Freund, S., Werthen, E., Dähne, S., Hühne, C.: Preliminary design of composite wings using beam-based structural models. In: German Aerospace Congress (DLRK) (Dresden, Germany, 2022). https://elib.dlr.de/188725/
28. Petsch, M., Kohlgrüber, D., Leon Munoz, C., Hecken, T., Balack, P., Atanasov, G., Silberhorn, D., Zerbst, D.: Analytical fuselage structure mass estimation using the pandora framework. In: German Aerospace Congress (DLRK) (Dresden, Germany, 2022). https://elib.dlr.de/192843/
29. Scholz, D.: Aircraft Design: Empennage Sizing. PDF. Aircraft Design. Lecture Notes by Prof. Dr. D. Scholz.. Hamburg University of Applied Sciences. Available from: http://LectureNotes.AircraftDesign.org (2015)
30. Sadraey, M.H.: Aircraft Design: A Systems Engineering Approach, 1^{st} ed. edn. John Wiley & Sons, Hoboken, New Jersey, USA (2012)
31. C. Bonnet and X. Barriola: Airbus Safety: Understanding Weight and Balance (2015). https://safetyfirst.airbus.com/understanding-weight-and-balance/1000/ Accessed 14 Oct (2024)
32. U.S. Air Force Stability and Control Digital DATCOM. Technical Report AFWAL-TR-83-3048, Air Force FDL, Wright-Patterson AFB, Ohio, USA (1978)
33. Air Accidents Investigation Branch: Serious incident: Airbus a321-231, g-wukg. Technical Report 10/2020, Department for Transport, United Kingdom (October 2020). AAIB Bulletin 10/2020. https://assets.publishing.service.gov.uk/media/5f5a0251d3bf7f7238f22fd2/Airbus_A321-231_G-WUKG_10-20.pdf
34. Jenatabadi, H.S., Ismail, N.A.: The determination of load factors in the airline industry. International Review of Business Research Papers **3**(4), 125–133 (2007)

Publisher's Note Springer Nature remains neutral with regard to jurisdictional claims in published maps and institutional affiliations.